Received: 12 May 2020 | Revised: 18 June 2020 | Accepted: 22 June 2020

DOI: 10.1002/cne.24973

RESEARCH ARTICLE

JCN RESEARCH IN SYSTEMS NEUROSCIENCE THE JOURNAL OF COMPARATIVE NEUROLOGY WILEY

Light adaptation mechanisms in the eye of the fiddler crab *Afruca tangeri*

Emelie A. Brodrick[1] | Nicholas W. Roberts[1] | Lauren Sumner-Rooney[2] | Christian M. Schlepütz[3] | Martin J. How[1]

[1]Ecology of Vision Laboratory, School of Biological Sciences, University of Bristol, Bristol, UK

[2]Oxford University Museum of Natural History, University of Oxford, Oxford, UK

[3]Swiss Light Source, Paul Scherrer Institute, Villigen, Switzerland

Correspondence
Emelie A. Brodrick, Ecology of Vision Laboratory, School of Biological Sciences, University of Bristol, Bristol BS8 1TQ, UK.
Email: e.brodrick@bristol.ac.uk

Funding information
The Royal Society, Grant/Award Numbers: RG150565, UF140558

Peer Review
The peer review history for this article is available at https://publons.com/publon/10.1002/cne.24973.

Abstract

A great diversity of adaptations is found among animals with compound eyes and even closely related taxa can show variation in their light-adaptation strategies. A prime example of a visual system evolved to function in specific light environments is the fiddler crab, used widely as a model to research aspects of crustacean vision and neural pathways. However, questions remain regarding how their eyes respond to the changes in brightness spanning many orders of magnitude, associated with their habitat and ecology. The fiddler crab *Afruca tangeri* forages at low tide on tropical and semi-tropical mudflats, under bright sunlight and on moonless nights, suggesting that their eyes undergo effective light adaptation. Using synchrotron X-ray tomography, light and transmission electron microscopy and in vivo ophthalmoscopy, we describe the ultrastructural changes in the eye between day and night. Dark adaptation at dusk triggered extensive widening of the rhabdoms and crystalline cone tips. This doubled the ommatidial acceptance angles and increased microvillar surface area for light capture in the rhabdom, theoretically boosting optical sensitivity 7.4 times. During daytime, only partial dark-adaptation was achieved and rhabdoms remained narrow, indicating strong circadian control on the process. Bright light did not evoke changes in screening pigment distributions, suggesting a structural inability to adapt rapidly to the light level fluctuations frequently experienced when entering their burrow to escape predators. This should enable fiddler crabs to shelter for several minutes without undergoing significant dark-adaptation, their vision remaining effectively adapted for predator detection when surfacing again in bright light.

KEYWORDS

Afruca tangeri, dark adaptation, fiddler crab, ophthalmoscope, rhabdom, synchrotron x-ray tomography, TEM

1 | INTRODUCTION

Many terrestrial animals must cope with light levels that vary from bright sunny skies to moonless nights a billion times dimmer (Warrant, 1999). Several different light- and dark-adaptation strategies have been described among members of the arthropods, the most successful animal phylum, which occupy an enormous diversity of visual niches on land (Stansbury & Moczek, 2013). These strategies

are as diverse as the optical architectures themselves, each highly specialized to suit the ecological needs and habitat of that animal. Fiddler crabs provide an excellent model for studying adaptations to light level fluctuations as they have evolved to forage during both the day and night, can be found in dense colonies on their mudflat habitats, and make a robust laboratory animal.

Fiddler crabs have large compound eyes and are highly dependent on vision in their behavioral ecology (Zeil & Hemmi, 2006). The morphology of their typical decapod apposition eye has been thoroughly described (Alkaladi & Zeil, 2014) for *Gelasimus vomeris*, and fiddler crabs are well-known for their distinctive scare-responses to a looming stimulus, making them ideal for behavioral experiments investigating crustacean vision (Hemmi, 2005; How et al., 2015). The West African fiddler crab, *Afruca tangeri* (synonymised from *Uca tangeri*, Eydoux, 1835; Shih, Ng, Davie, et al., 2016) is abundant and widespread on southwest European and northwest African coastlines (Wolfrath, 1993). Fiddler crabs, including *A. tangeri*, have been studied by those researching aspects of crustacean polarization vision (How, Pignatelli, Temple, Marshall, & Hemmi, 2012; Smithers, Roberts, & How, 2019), color vision (Detto, 2007; Falkowski, 2017; Jordão, Cronin, & Oliveira, 2007), and visually-guided behavior (Altevogt & von Hagen, 1964; Barnatan, Sztarker, & Tomsic, 2019; Cummings, Jordão, Cronin, & Oliveira, 2008; Latruffe, McGregor, & Oliveira, 1999; Oliveira & Custódio, 1998). Experiments utilizing thresholds of visual sensitivity as a response variable are commonplace in these studies. However, crucial information was missing on how fiddler crabs adapt to large fluctuations in brightness and whether their adaptive mechanisms are controlled by a circadian clock. Considerations such as ambient light exposure before or during experiments, and the time of day crabs are tested, may have substantial impacts on their ability to detect an experimental visual stimulus.

A. tangeri are mostly active on diurnal low tides when they emerge from burrows to forage in dense groups on the mudflat surface. They have highly visual lifestyles, frequently engaging in visually-dependent intraspecific social interactions while constantly monitoring their surroundings for potential predators (Zeil & Hemmi, 2006). The eyes wrap almost fully around the eyestalks and are held high above the head, providing a panoramic field of view (Bagheri et al., 2020; Smolka & Hemmi, 2009). During daytime, they are exposed to bright tropical sunlight and strong reflected glare from the mudflat surface. In summer, when surface temperatures remain higher than 18°C after sunset, *A. tangeri* also remain active on the mudflat at night (Altevogt & von Hagen, 1964; von Hagen, 1962; Wolfrath, 1993). From our own observations (Figure 1) during breeding periods, males continue to wave their major chelipeds for at least 2 hr after sunset, a behavior used to visually signal to potential mates (Oliveira & Custódio, 1998). This suggests that effective vision is also possible in very dim light and led us to the hypothesis that this species undergo considerable adaptation between day and night to cope with the large changes in available light levels, spanning 10 orders of magnitude.

A common mechanism for adaptation to light level fluctuations in compound eyes is migrations of mobile screening pigment granules within the photoreceptors or in adjacent pigment cells

FIGURE 1 Three *A. tangeri* males signaling visually by waving their large white claws to attract female conspecifics in very dim light ~1 hr after sunset. Image taken from a video using an infrared dim light vision camera [Color figure can be viewed at wileyonlinelibrary.com]

(Land & Nilsson, 2012; Meyer-Rochow, 2001). Pigment cells are usually located distally where the crystalline cone and rhabdom meet, and/or proximally, near the basement membrane. Screening pigment granules within photoreceptors may move either longitudinally or radially toward the light path, to protect the microvilli, where phototransduction occurs, from over-exposure and excess light damage (e.g. King & Cronin, 1994a, 1994b). In dim light, the pigment recedes, boosting sensitivity by allowing more light to reach the photoreceptors. There is great diversity of screening pigment populations, distributions and their movements among the crustaceans, even within closely related groups (Brown, 1961), including several crab species that are reported to use pigment migrations as a light-dark-adaptation strategy (Eguchi & Waterman, 1967; Fingerman, 1970; Ludolph, Pagnanelli, & Mote, 1973; Leggett & Stavenga, 1981; Arikawa, Kawamata, Suzuki, & Eguchi, 1987; Vargas et al., 2010; De Moraes Vaz Batista Filgueira, Guterres, De Souza Votto, et al., 2010).

Slower circadian changes may alter light sensitivity by changing the volume of the photoreceptor cells via a widening or lengthening of the rhabdom, increasing the surface area where phototransduction can occur. There are several intertidal crab species for which this has been identified as the primary dark-adaptation mechanism (Arikawa et al., 1987; Blest, Stowe, & Price, 1980; Nässel & Waterman, 1979; Stowe, 1981, 1983), but although some species were well-researched in the late 1960s to late 1980s, there is no information on fiddler crabs.

Ophthalmoscopy provides a useful tool for visualizing changes in the living eye associated with light-adaptation (Stowasser, Owens, & Buschbeck, 2017). When illuminating a compound eye, a black spot or pseudopupil can often be seen where the optical axes of the ommatidia are in line with the observer (Franceschini, 1972). Focussing a camera deeper within the eye on the distal tip of the fused rhabdom of an apposition eye produces a superimposed image of the combined apertures of several neighboring ommatidia (Ro & Nilsson, 1993). This is known as the "deep pseudopupil," the centre of which is dark due to the light-absorbing central rhabdoms, surrounded by a ring of more reflective screening pigment cells. Changes in the appearance and shape of the deep pseudopupil can be measured to visualize the

associated pigment migrations or increases in acceptance angles and photoreceptive area, in response to light level changes.

In the present study, we describe the structural mechanisms of light- and dark-adaptation in *A. tangeri* using a variety of complementary approaches. From transmission electron micrographs (TEMs) and light micrographs, we characterize the screening pigment distributions in the eye and compare anatomical dimensions of the photoreceptors and crystalline cones, between day and night in light- and dark-adapted eyes. Synchrotron X-ray tomography of eyes fixed at midday and midnight allow visualization and measurement of these changes across the whole eye in three dimensions. We also take advantage of the direct correlation between deep pseudopupil width and the aperture size of an individual ommatidium, by using a custom ophthalmoscope to measure physiological changes in acceptance angle during dark adaptation in the living eye.

2 | MATERIALS AND METHODS

2.1 | Eye sample preparation

Male and female fiddler crabs *(A. tangeri)* were collected from mudflats in El Rompido (Andalucía, Spain, 37°13′02.3″N, 7°07′08.1″W) during low tide and kept in containers with 1–2 cm seawater for 48 hr maximum. The animals were separated into experimental treatments and preadapted to the desired light level for an appointed time (Tables 1 and 2). Both eyes were dissected by cutting the connective tissue at the base of the eyestalk using a razor blade dipped in fixative, a method which best preserves the eye structures (Alkaladi & Zeil, 2014). Animals were euthanized immediately by severing the thoracic and cerebral ganglia. A dim lamp behind a red filter removing wavelengths <600 nm, (No.027, Lee Filters, Andover, UK) provided enough illumination to dissect the dark-adapted eyes of crabs in the darkroom without altering their adaptation state (irradiance spectrum in Supporting Information). Eyes were placed directly into chilled fixative containing 2.5% glutaraldehyde and 4% paraformaldehyde in 2× PEMS buffer (adapted from Chiou, Cronin, Caldwell, & Marshall, 2005).

The chitinous eyestalk was carefully removed from the eye tissue in fixative using a dissection microscope in a brightly lit room for light-adapted eyes, or a darkroom under dim red light for dark-adapted eyes. After spending at least 3 days in a refrigerator, the fixed eyes were washed in PEMS buffer, stained with 2% osmium tetroxide, and dehydrated with increasing concentrations of graded ethanol, then washes of propylene oxide. The samples were then infiltrated and embedded in EPON resin blocks and polymerized in an oven (60°C for 48 hr).

TABLE 1 Experimental treatments used to investigate rates of rhabdom cross-sectional area changes during light and dark-adaptation processes

Treatment	Sample time	Preadaptation method
Day light-adapted	12:00	Kept under natural sky conditions from sunrise until midday
Night light-adapted	00:00	Kept under natural sky conditions during daylight hours, then moved just before dusk under bright controlled LED lighting to prolong light-adaptation after sunset
Day dark-adapted	12:00	Dark-adapted just before dusk by housing in a light-tight container within a darkroom, remaining there until midday the following day
Night dark-adapted	00:00	Dark-adapted just before dusk by housing in a light-tight container within a darkroom, remaining there until midnight

2.2 | Transmission electron microscopy

Ultrathin (70 nm) sections from the lateral-facing eye equator region were cut with a diamond knife (DiATOME, Hatfield, UK) on an ultramicrotome (EM-UC6, Leica, Wetzlar, Germany) and poststained with 3% uranyl acetate and lead citrate. Transverse sections were cut through the primary pigment cell (PPC) layer allowing measurement of the region where the crystalline cone tip gives way to the distal tip of the R8 rhabdom. Here, cross-sectional area of the light path is at its smallest and acts as an aperture for light passing through the primary pigment layer. Thin sections were imaged using a TEM (Tecnai 12, 120 kV BioTwin Spirit, FEI Company, Hillsborough, FL). Using the Fiji-ImageJ software (Schindelin et al., 2012), cross-sectional areas of 10 apertures per eye were measured in this region, as well as diameter of the pupillary opening in the PPCs surrounding this aperture, measured as the shortest distance between two pigment granules in PPCs on opposite sides of the aperture.

Further sections were cut deeper inside the eye exposing the rhabdom of R1-7 photoreceptor cells in transverse profile just proximal to their nuclei. From 16 sample TEMs of ommatidia from the lateral-facing equatorial region of each eye, the cross-sectional areas of rhabdoms were measured with the Fiji-ImageJ (Schindelin et al., 2012). These TEMs were additionally analyzed for screening pigment granule distributions. After conversion to binary images using the "Threshold" function in Fiji-ImageJ, they were processed with MorphoLibJ plugins "Watershed" and "Fill Holes" (Legland & Andrey, 2016). The inbuilt function "Analyze Particles" quantified pigment granules, excluding those in the cell soma not associated with the palisade vacuoles. The number of granules within the palisade bridges were counted as a proportion of the total surrounding the palisade/rhabdom area.

2.3 | Light microscopy

During sectioning of the EPON blocks for TEM, semithin (1,500 nm) sections were also cut, stained with methylene blue and mounted

TABLE 2 Experimental treatments used to investigate rates of rhabdom cross-sectional area changes during light and dark-adaptation processes

Treatment	Sample times	Preadaptation method	Sampling method
Daytime: dark to light	12:00–14:00	Six crabs dark-adapted just before dusk in a light-tight box within a darkroom and remained there overnight	From 12:00 the following day, eyes were collected from one dark-adapted individual, and then from the other five individuals 10, 20, 30, 60, and 120 min after sudden exposure to LED light
Daytime: light to dark	12:00–15:00	Seven crabs were light-adapted under bright controlled LED light from dawn onward	At 12:00, five individuals were placed inside a light-tight box in a darkroom. Eyes were sampled after 15, 30, 60, 120, and 180 min of darkness. The other two crabs remained light-adapted and were sampled at 12:00 and 15:00
After sunset: light to dark	21:00–00:00	Seven crabs were light-adapted under bright controlled LED light from dawn onward	At 21:00 five individuals were placed inside a light-tight box in a darkroom and sampled after 15, 30, 60, 120, and 180 min of darkness. The other two crabs remained light-adapted and were sampled at 21:00 and 00:00

on glass slides. Images were collected with a light microscope (Leica DM750) and distributions of PPC pigments were examined. From six midday light-adapted eyes and six midnight dark-adapted eyes, additional sections were cut horizontally through the eye equator to expose whole ommatidia in longitudinal section. From light micrographs of these sections, crystalline cone and rhabdom lengths of six lateral-facing ommatidia were measured using the Fiji-ImageJ (Schindelin et al., 2012).

2.4 | Synchrotron X-ray tomography

Eyes from two male crabs of equal body size were dissected and fixed in 2.5% glutaraldehyde and 4% paraformaldehyde in 2× PEMS buffer, one naturally light-adapted at midday and the other dark-adapted at midnight. Using synchrotron X-ray microtomography, the samples were scanned at the TOMCAT beamline, Swiss Light Source (Paul Scherrer Institute, Switzerland; Stampanoni, Groso, Isenegger, et al., 2006), once under 40× combined magnification and again under 4× magnification, giving effective voxel sizes of 163 and 1,625 nm, respectively. The samples were scanned with a monochromatic 12 keV beam, using a 20 μm thick LuAG:Ce scintillator, exposure time of 380 ms and a propagation distance of 12 mm. Two thousand projections were recorded as the sample rotated through 180°. The radiographic projections were reconstructed into aligned tiff image stacks and Paganin filtered (delta = 1^{-7}, beta = 1^{-9}; Paganin, Mayo, Gureyev, Miller, & Wilkins, 2002) using custom in-house software (Marone & Stampanoni, 2012). These 3D reconstructed volumes were cropped and segmented using Avizo 8.0 (ThermoFisher Scientific, Waltham, MA). Features such as the cornea, crystalline cones, PPCs, and rhabdoms were segmented and measured. Two whole-eye scans were used to count the approximate number of ommatidia by sampling 10 representative areas per eye and multiplying facet count by total eye surface. External and internal dimensions of the eye were measured, including area of eye tissue occupied by crystalline cones and photoreceptors, and the lengths of these cells across the eyes.

2.5 | Ophthalmoscopy

An ophthalmoscope was constructed to visualize changes associated with dark adaptation in the deep pseudopupil of living fiddler crabs. The apparatus incorporated a UI-3590CP-C-HQ-R2 camera with CMOS color sensor (Imaging Development Systems, Obersulm, Germany), 10× objective lens (Plan N, Olympus, Tokyo, Japan), beam-splitter (Thorlabs, Newton, MA) and a light source with halogen and deuterium bulbs (Mikropack DH-2000), that provided both a coaxial adapting light and imaging light (apparatus diagram in Supporting Information).

Six adult crabs (three females, three males) with carapace width of 16–19 mm were used in this experiment. Crabs were temporarily tethered, one at a time, to a post held by a micromanipulator via a small polypropylene disk fixed to their carapace with cyano-acrylate glue. Claws were carefully wrapped and held close to the body with electrical tape to help immobilize the crab and prevent it reaching the apparatus. One eye was held in its usual upright position using a small dab of cyano-acrylate glue on the back of the eye stalk, attached to a small wooden stick. The crab was submerged in a small glass tank of seawater lined externally with black felt to remove external illumination, except for a small window of quartz glass. Through this, the ophthalmoscope was positioned to image the front of the eye.

The camera was focused on the deep pseudopupil while illuminated with coaxial and broad-field light. Then with just coaxial illumination, an image was taken of the light-adapted eye. This light was subsequently switched off and the crab was left to dark-adapt. After a period of either 15, 30, 60, or 180 min in darkness, the coaxial illumination was switched on and an image collected within 75 ms of light exposure. Another image was collected after a further 10 s, to look

for evidence of fast pigment reactions to sudden bright light exposure. All six crabs were tested at these four different time points during adaptation to darkness during both daytime (11:25–18:50) and after sunset (20:28–00:54). Only one test per crab was conducted during the evening to avoid excessive unnatural disruption of the circadian light-dark cycles.

The edges of the deep pseudopupil were determined in Fiji-ImageJ by drawing a horizontal line across the middle at its widest point, and using the inbuilt "Plot Profile" function to produce a histogram profile of greyscale values against distance along the line. The intensity profiles were characterized by two maximum peaks in intensity (the pigment cells) either side of a central minimal trough (the dark rhabdom). The distance across this trough (along the *x*-axis) was considered the deep pseudopupil and its width was compared to the equivalent image taken just before dark-adaptation.

2.6 | Statistical analysis

Statistical tests were performed using the R software (version 3.5.1; http://www.R-project.org/). Following Kolmogorov–Smirnoff tests for normality and Bartlett's test for homogeneity of variances, statistical analyses to compare physiological measurements between adaptation states were performed using the R package "onewaytests" (Dag, Dolgun, & Konar, 2018). Where these assumptions were met, Student's *t*-test (for comparison between two groups) or Analysis of variance (ANOVA, to compare four treatments) were used. Threshold probability (alpha) values were set to .05 throughout. For data with unequal variances, Welch's test was used instead. Following ANOVA, post hoc pairwise comparisons tests were performed using TukeyHSD (or Bonferroni corrections when using Welch's test).

3 | RESULTS

3.1 | General anatomy

The apposition compound eyes of *A. tangeri* (Figure 2a–c) are of typical crustacean design and the following descriptions pertain to both light and dark-adapted states. Eye anatomy was found to be indistinguishable from *G. vomeris*, another fiddler crab described in detail by Alkaladi and Zeil (2014). Each eye contains ~10,000 ommatidia (approximated from whole-eye synchrotron tomograms from two adult male crabs, carapace width 25 mm), which consists of a flat corneal lens and crystalline cone (made from four cells, Figure 2d,e) that direct light on to the rhabdom. The secondary pigment cells (SPCs) matched the detailed description given of *G. vomeris* (Alkaladi & Zeil, 2014), changing in morphology and pigment content across the eye. Anchored to the corner of each hexagonal corneal lens, long thin SPC processes stretch down the length of the crystalline cones to the PPCs below (Figure 2d,e). In the dorsal eye these contain the nucleus and brown screening pigment granules, presumably to screen excess skylight from above. In equatorial and ventral eye regions these distal processes are empty of pigment granules (Figure 2d, arrows) and the proximal cell bodies contain the nucleus plus an assortment of pale reflective pigment granules. The narrow T-shaped soma reaches up and down the eye in a dorso-ventral (vertical) direction (Figure 2a,e), covering the dark PPCs below with a more reflective layer, giving the eye it's color. Below, the narrow proximal tip of each crystalline cone is surrounded by four PPCs forming a dense and highly absorbent screening layer (Figure 2f). Very thin extensions of these cells reach down between the ommatidia toward the basement membrane. Within the PPC layer, the crystalline cone meets the distalmost rhabdom of R8 (Figure 2g,h), a four-lobed UV-sensitive photoreceptor cell with disordered microvilli (Figure 2h,i). The remaining majority of the ommatidium's length is formed by seven long photoreceptor cells, R1–7, arranged in a ring around a central rhabdom (Figure 2j), to which they contribute vertically (R1, R2, R5, and R6) and horizontally (R3, R4, and R7) orientated microvilli, facilitating sensitivity to the polarization of light (Figure 2k; Alkaladi & Zeil, 2014; How et al., 2015). There are at least two populations of "soma" pigment granules distributed throughout the distal part of the photoreceptor cells, most densely around the nuclei. Proximal to the nuclear region, extending to the basement membrane (the majority of the rhabdom's length), a third population of electron-dense pigment granules tightly encircles the palisade vacuole, forming a distinctive ring around the rhabdom. There are no proximal pigment cells above the basement membrane in this species.

3.2 | Screening pigment distributions

Ignoring the "soma" pigment granules largely associated with nuclei in the distal part of R1–7 cells, many of the screening pigment granules were distributed in a ring around the outside the palisade vacuoles surrounding the rhabdom in all adaptation states (Figure 3). Very few granules were located inside the cytoplasmic bridges of the palisade vacuoles in light-adapted eyes, or any treatment (Table 3). There were slightly more pigment granules within bridges in light-adapted eyes than dark-adapted eyes, especially during daytime; however, this was still a small number (1.9 ± 1.8 granules per image); 4.3% of the total granules. When light-adapted, pigment distributions did not resemble that of a mantis shrimp, *Gonodactylus oerstedii*, in which radial pigment migrations are known (King & Cronin, 1994b). On an observational note, in daytime the palisade of light-adapted eyes appeared less "solid" with more numerous and wider bridges than other conditions.

Light microscopy (Figure 4a), and synchrotron X-ray tomography (Figure 4b) revealed that pigment granules within PPCs did not appear to migrate as there was no change in cell appearance or shape between light- and dark-adapted states, or day and night. The pigment appeared consistently in a dense layer surrounding the region where the narrow crystalline cone tips meet the distal R8 cell in all eyes examined.

Due to the low contrast pigment and thin string-like shapes of the SPCs, they appeared irregularly on sections, if at all, and were

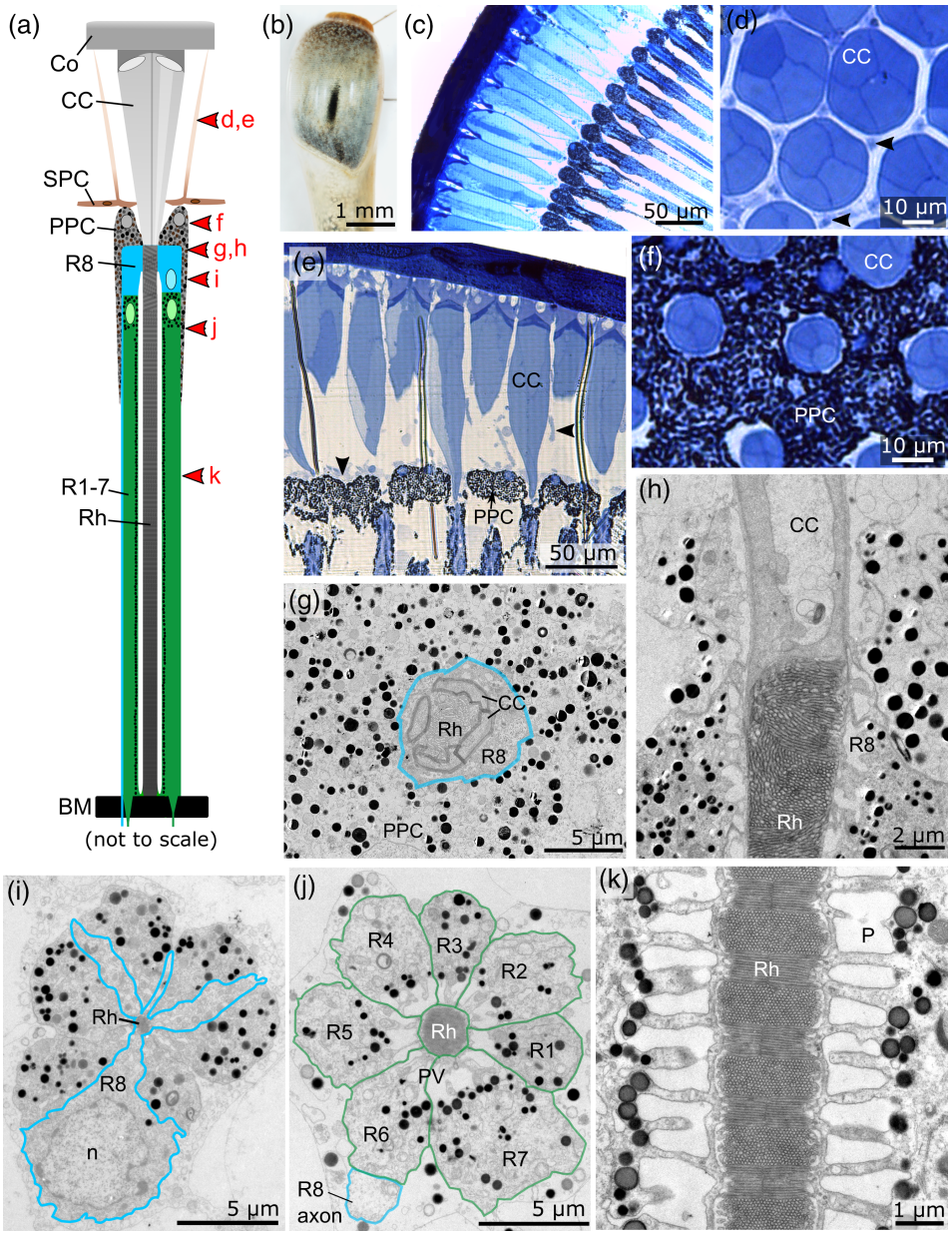

FIGURE 2 Anatomy of the *Afruca tangeri* eye shown in TEMs and light micrographs (stained blue) of both longitudinal (LS) and cross sections (XS) of ommatidia from equatorial eye regions (light-adapted, daytime). (a) Illustration of an ommatidium in LS with main structures labeled including the cornea (Co), crystalline cone (CC), primary (PPC) and secondary (SPC) pigment cells and basement membrane (BM). The photoreceptor cells R8 (blue), and R1–7 (green) contribute microvilli to a central rhabdom (Rh). Cell nuclei shown in their relative positions. Red arrows indicate the corresponding locations of images d-k along an ommatidium. (b) Photograph of a whole eye, frontal view. (c) Horizontal section across the eye equator showing rows of ommatidia under the corneal surface. (d) Crystalline cones in XS showing their four component cells surrounded by six SPC extensions (arrows), empty of pigment. (e) The distal part of several ommatidia, LS, showing their crystalline cones stretching between the cornea and PPC layer; SPCs indicated by arrows. (f) Primary pigment cell layer in XS surrounding CC tips. (g) The distal R8 cell (outlined blue), where CC tips intersect with the start of the rhabdom in XS, forming a narrow aperture. (h) Same location as g showing CC and rhabdom intersection in LS. Note disordered rhabdom. (i) R8 cell (outlined blue) in XS showing its four lobed design and nucleus (n) intersected with pigmented tips of R1-7 cells. (j) R1–7 photoreceptor cells (outlined green) in XS just proximal to the nuclei (location sampled for comparative rhabdom measurements). (k) Rhabdom in LS from a dark-adapted eye, midday, showing the ordered bands of microvilli, ringed by palisade vacuoles (P) and screening pigment granules [Color figure can be viewed at wileyonlinelibrary.com]

invisible in synchrotron scans. Therefore, we were not able to make meaningful measurements of the cells or reliably compare positions between treatments. However, there were no obvious conspicuous changes from general observations.

3.3 | Crystalline cone aperture

From TEM images within the PPC layer, the cross-sectional area of the light-transmissive crystalline cone aperture changed as a function

of the adaptation state (Welch's ANOVA, $F_{[3,10.5]}$ = 18.4, p < .001, n = 6; Figure 5a–c). Pairwise comparisons (using Bonferroni corrections) revealed that apertures were narrower when light-adapted, significantly more so at midday (mean area 2.9 ± 1.1 μm^2) than at midnight (6.3 ± 1.6 μm^2) (p = .01). At midday, apertures in dark-adapted eyes (5.3 ± 1.8 μm^2) were similar in area to apertures in the light-adapted eyes (p = .14). At midnight, however, dark-adapted crabs had aperture areas of 20.9 ± 6.2 μm^2, significantly larger (by almost four times) than dark-adapted crabs at midday (p < .001).

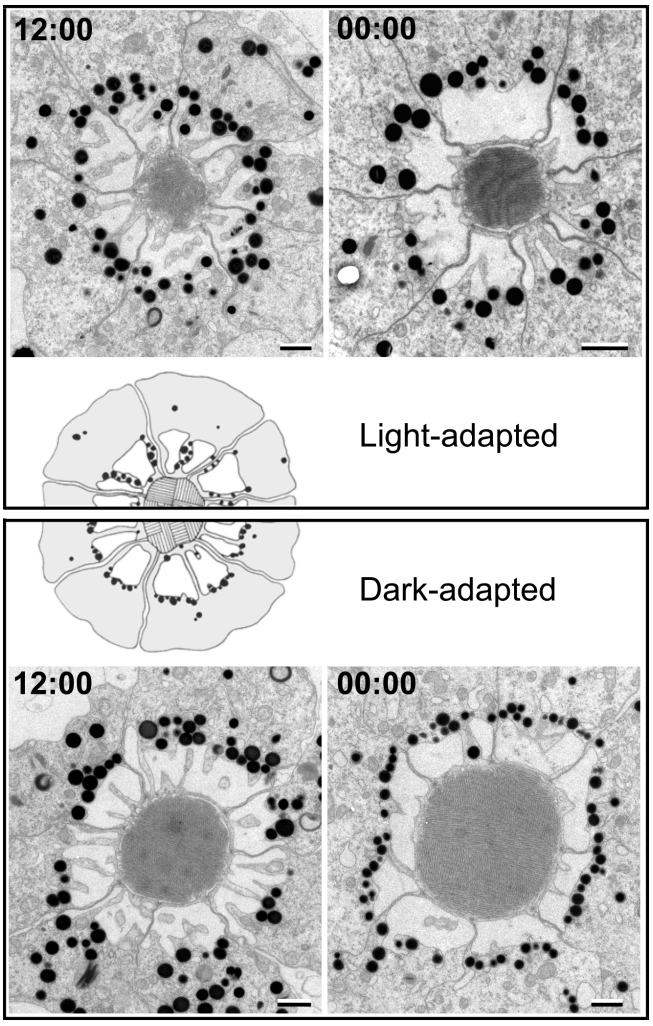

FIGURE 3 Typical arrangements of screening pigment granules observed with TEM in light- and dark-adapted *Afruca tangeri* eyes at midday and midnight (ommatidia in XS). The central rhabdoms are surrounded by palisade vacuoles (white) perforated with cytoplasmic bridges. Distributions of black pigment granules in light-adapted *A. tangeri* eyes did not match the central hypothetical diagram of radial pigment migrations in *Gonodactylus oerstedii* (adapted from King & Cronin, 1994b), but resembled the dark-adapted state instead. One or two granules were occasionally located inside the bridges nearer the rhabdom, but the majority bordered the palisade. All scale bars = 1 μm

The diameter of the pupillary opening between PPCs (surrounding an aperture) was also measured (Figure 5a), indicated by dashed line in Figure 5b. Differences between treatment groups were small, but there was a significant effect of adaptation state (ANOVA, $F_{[3,236]}$ = 7.27, p < .001). Pairwise comparisons (Tukey tests) between groups showed that mean pupil diameters in dark-adapted eyes at midnight were slightly larger than the other three treatments (p < .011), with mean value 7.0 ± 1.3 μm. However, this difference was due to wide diameters from just three individuals in this group; the other three crabs had similar diameters to other treatments. Pupillary openings between pigment cells of the dark-adapted crabs at midday (6.2 ± 0.6 μm) and light-adapted eyes at midday (mean value 5.8 ± 0.5 μm) and midnight (6.0 ± 0.6 μm) did not differ from one another significantly when compared with pairwise Tukey tests (p = .608–.974).

3.4 | Deep pseudopupil

The deep pseudopupil appeared as an elongated dark centre (the light-absorbing rhabdoms) surrounded by a brighter ring (the reflective pigment cells). The deep pseudopupils of six individuals expanded in size during dark adaptation in both daytime and after sunset (example in Figure 6a); however, the rate and extent to which this occurred was much greater after sunset, both in proportionate and absolute measures. In a fully light-adapted state, it was significantly wider after sunset (137.1 ± 11.0 μm) than during the day (108.7 ± 4.0 μm; T_5 = −6.0, p < .05) (Figure 6b). In daytime, the pseudopupil width increased by 21.5% during 3 hr of darkness. It had grown to its maximum size after 60 min of dark adaptation, as mean widths at 60 and 180 min were not significantly different to one another (Student's t-test, t_5 = −1.2, p = .12). At night, the pseudopupil grew much wider during dark-adaptation and continued to significantly increase between 60 and 180 min (Student's t-test, t_5 = −3.3, p = .004), resulting in a total width increase of 56.4% in the 3 hr period.

After 10 s of bright light exposure following these varying dark adaptation periods there was no measurable reduction in deep pseudopupil width, or any change in general appearance in the eye during both daytime and evening (Figure 6c). This suggests that no pigment migrations or any other visible change to alter the acceptance angle of

TABLE 3 Mean number of screening pigment granules per ommatidium (± standard deviation) associated with the rhabdom and palisade vacuoles, counted in 15 ommatidia from each individual eye in different adaptation states

Treatment (n = 8)	Total granules	Within bridges	% within bridges
Day light-adapted	47.3 ± 9.7	1.9 ± 1.8	4.3
Night light-adapted	51.9 ± 19.2	0.3 ± 0.4	0.7
Day dark-adapted	38.4 ± 10.9	0.0 ± 0.1	0.1
Night dark-adapted	51.5 ± 17.5	0.1 ± 0.1	0.1

Note: Number of granules within cytoplasmic bridges of the palisade is also shown as a proportion of the total.

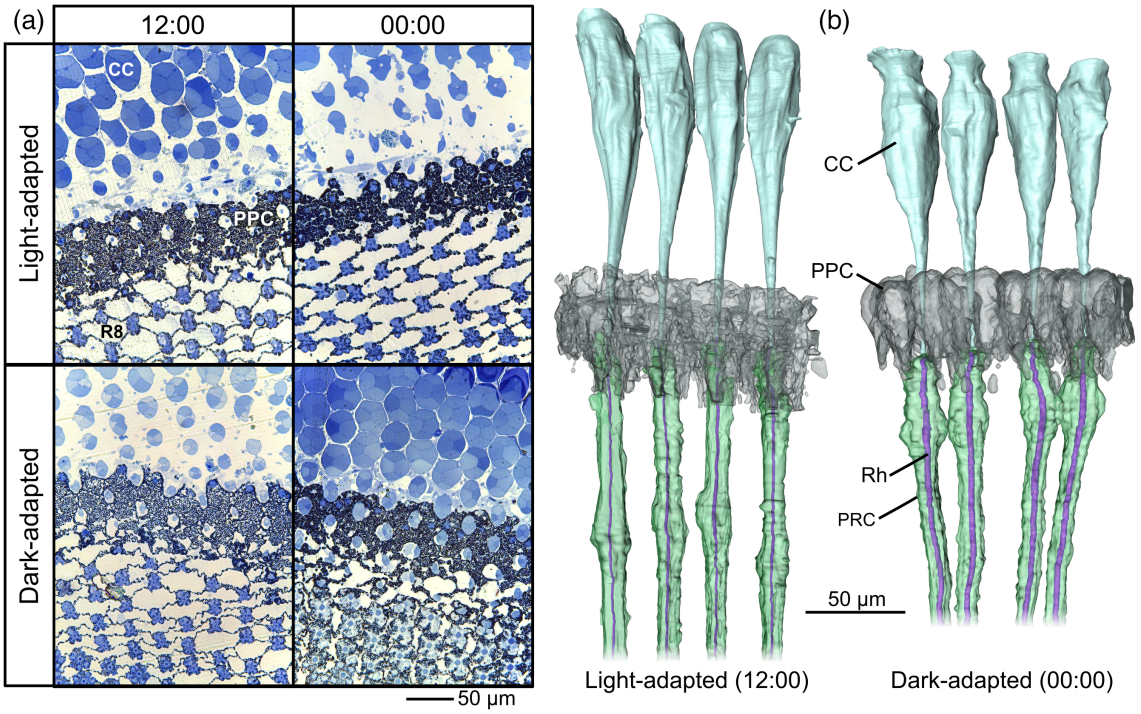

FIGURE 4 (a) Light micrographs of oblique sections through the primary pigment cell layer in light-adapted and dark-adapted *Afruca tangeri* eyes at midday and midnight. The primary pigment cell layer (PPC) appears as a dark band between crystalline cones (CC) and R8 cells (R8), remaining similar in appearance in all conditions. Secondary pigment cells appear as pale streaks/small dots above the PPCs. (b) Segmented X-ray tomograms of four ommatidia from a light-adapted eye at midday (left) and a dark-adapted eye at midnight (right). The PPCs surround the region where crystalline cones meet the photoreceptor cells (PRC) with central rhabdoms (Rh) in both eyes, with similar pigment distributions (animated version of tomograms in Supporting Information) [Color figure can be viewed at wileyonlinelibrary.com]

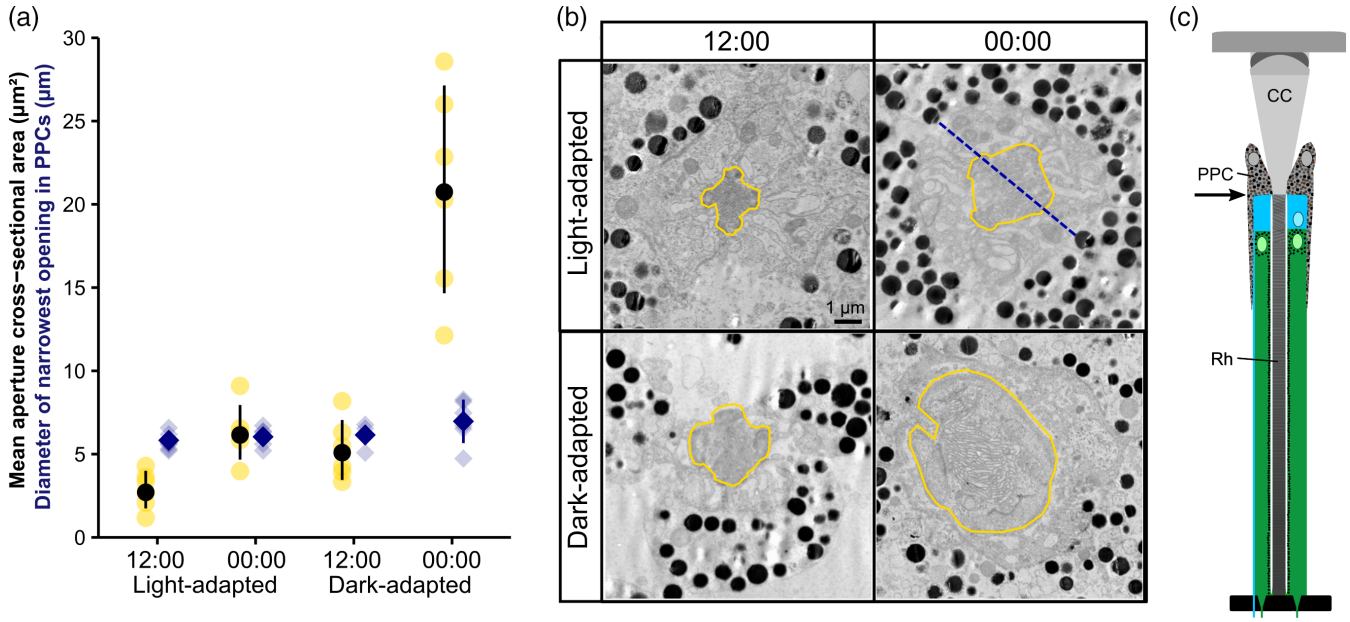

FIGURE 5 (a) Cross-sectional area of the crystalline cone tip aperture within the primary pigment layer in light-adapted and dark-adapted eyes, at midday and midnight. Circular yellow points represent individual means (n = 6); black filled circles show global means with standard deviation bars. Plotted alongside are mean diameters of the pupillary opening between primary pigment cells, which surround the aperture. Individual means (blue diamonds) and global mean (navy diamonds) are displayed with standard deviation bars. (b) Representative TEM examples of crystalline cone tip apertures (outlined in solid yellow) for each adaptation state, each measuring close to the mean for that treatment, for visual comparison. The navy dashed line in the top right TEM exemplifies the pupillary opening (shortest measured distance between two opposite pigment granules). (c) TEM sample location indicated by black arrow on ommatidium diagram [Color figure can be viewed at wileyonlinelibrary.com]

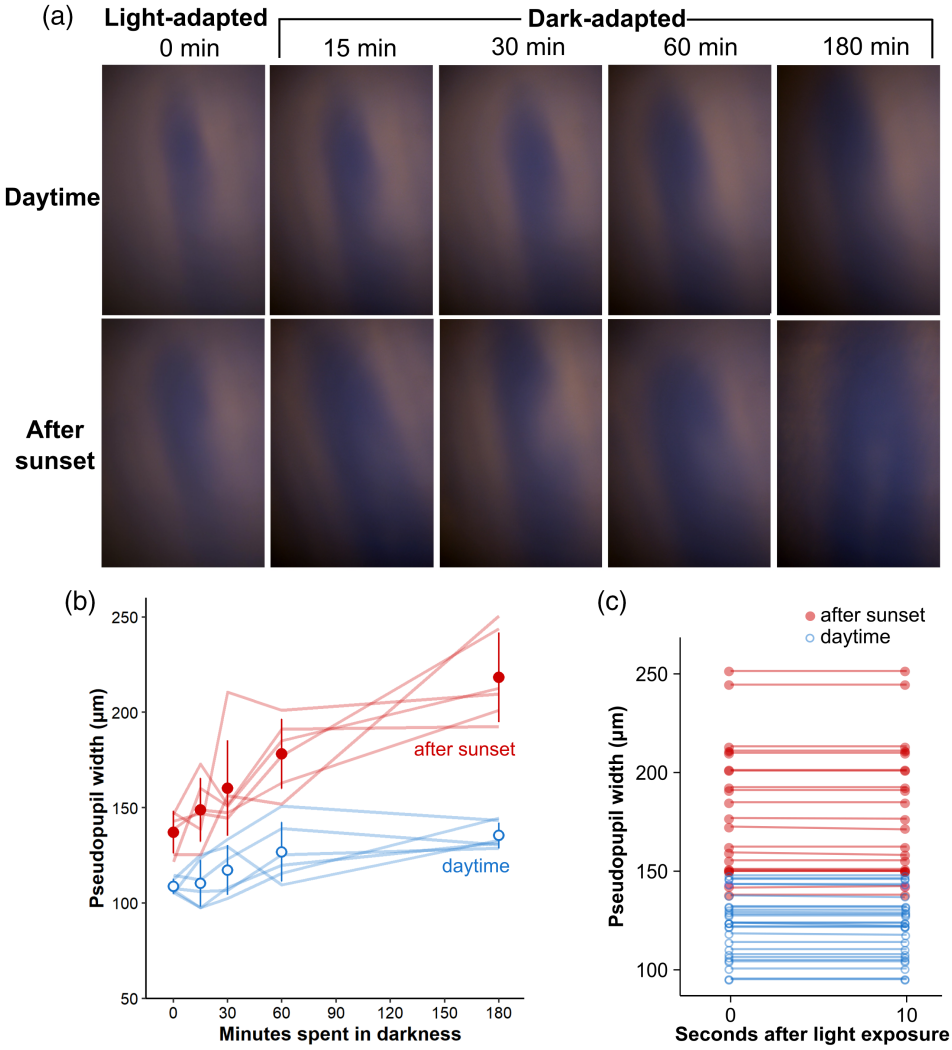

FIGURE 6 (a) Ophthalmoscope images of the deep pseudopupil of a single crab (*Afruca tangeri)* after varying periods adapting to darkness during daytime and after sunset. (b) Width measurements of the deep pseudopupil, as fully light-adapted eyes (0 min) spend varying periods (15–180 min) adapting to darkness. Lines show data for each individual crab (n = 6) during daytime (blue) and after sunset (red) and mean widths represented by open/filled points ± standard deviation bars. (c) Deep pseudopupil width at the moment the dark-adapted eye is first exposed to bright light (0 s), and again after 10 s of light exposure, during daytime (blue open points) and after sunset (red filled points). Lines link pairwise individual measurements [Color figure can be viewed at wileyonlinelibrary.com]

the ommatidia occurred in reaction to bright light, within the time-frame of 10 s.

3.5 | Rhabdom widening

Cross-sectional rhabdom areas differed between adaptation states (Welch's ANOVA, $F_{[3,14.4]}$ = 56.91, p < .001, n = 8; Figure 7) and pairwise comparisons showed that all combinations differed significantly from one another (Bonferroni correction, p < .05). Dark-adapted crabs at midnight had significantly wider rhabdoms (mean area 18.4 ± 4.5 µm^2) than all other treatments, including by a factor of ~2.6, the daytime dark-adapted crabs (7.1 ± 1.0 µm^2). Light-adapted crabs at midday had the narrowest rhabdoms (3.3 ± 0.4 µm^2), exceeded slightly by midnight light-adapted crabs (4.3 ± 0.3 µm^2). Therefore, the cross-sectional rhabdom area appears to change by a factor of 5.6 during a typical 24-hr period, in *A. tangeri*.

Individual crabs (n = 1) were also sampled at various time points during dark- and light-adaptation (Table 2, Figure 8) to assess the approximate timescales over which the cross-sectional areas of their rhabdoms grow and narrow.

3.5.1 | Light to dark

After sunset, from the narrow rhabdom of the light-adapted crab (mean area 3.0 µm^2), crabs undergoing dark-adaptation had progressively wider rhabdoms, with area of 8.2 µm^2 after just 15 min in the dark, up to a maximum size of 19.7 µm^2 after 1 hr. Rhabdoms sampled at 2 and 3 hr into dark adaptation were not widened beyond this. During daytime, rhabdom widening also appeared to reach completion within 1 hr of darkness; however, growth was minimal. The largest rhabdom area was just 4.5 µm^2. Fully light-adapted crabs (n = 1) were additionally sampled at the same time (15:00 and 00:00) as the 3-hr dark-adapted crabs, to show that rhabdoms do not widen over this circadian period in the absence of darkness.

3.5.2 | Dark to light

From the dark-adapted crab's mean rhabdom measurement of 6.2 µm^2 at midday, crabs sampled after 10, 20, and 30 min bright light exposure had progressively narrowed rhabdoms, down to a minimum of 3.4 µm^2 at 30 min. Longer light exposure periods (1 and 2 hr) did not result in narrower rhabdoms than this.

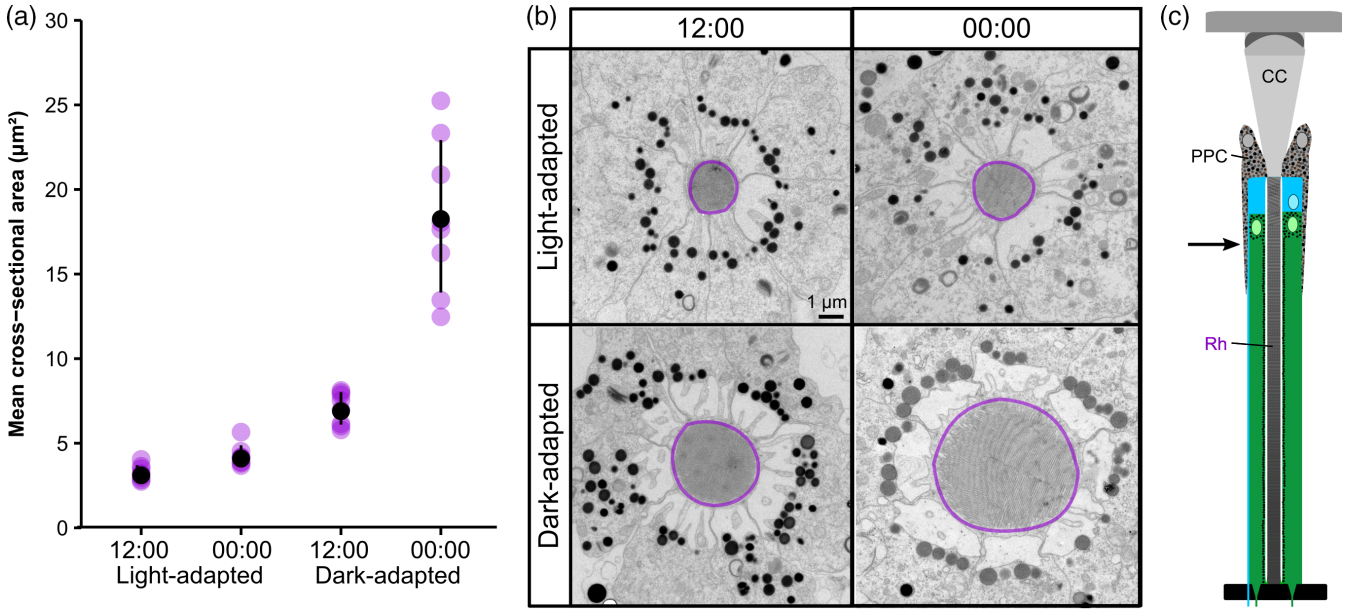

FIGURE 7 (a) Cross-sectional rhabdom areas of light-adapted and dark-adapted *Afruca tangeri* eyes, at midday and midnight. Purple points represent individual means (n = 8); global means shown by black points ± standard deviation bars. (b) Representative TEMs of ommatidia when light-adapted and dark-adapted, at midday and midnight. Each rhabdom (outlined purple) approximates to the mean cross-sectional area for the crabs in that treatment, allowing visual comparison. (c) TEM sample location indicated by black arrow on ommatidium diagram [Color figure can be viewed at wileyonlinelibrary.com]

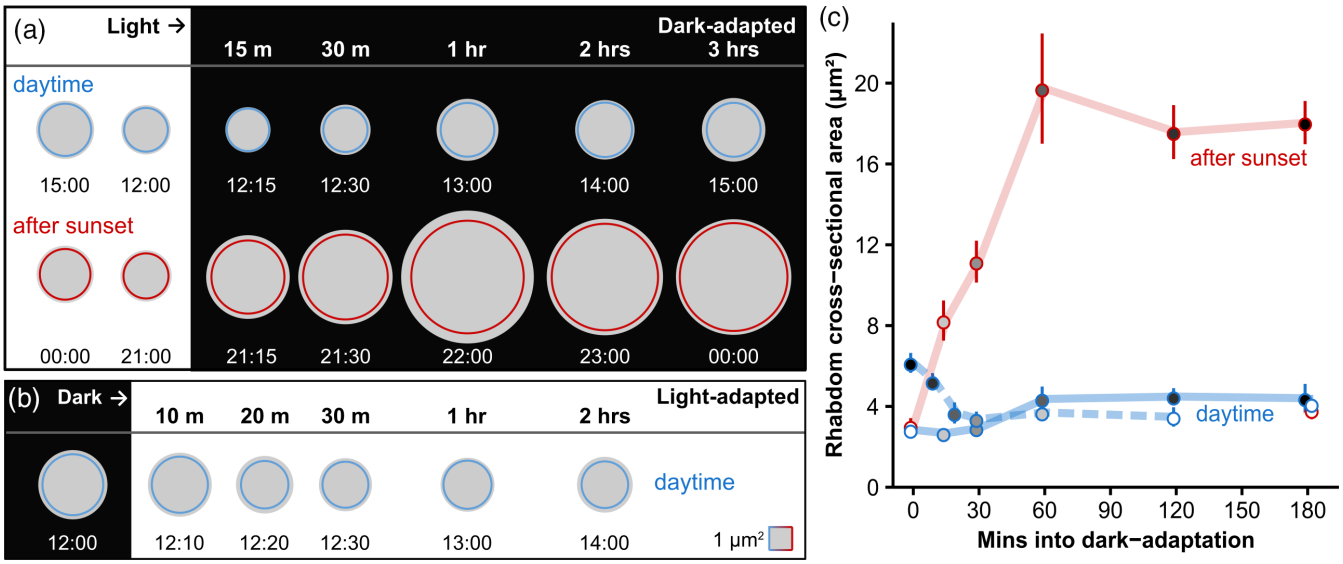

FIGURE 8 Scaled gray circles represent relative cross-sectional areas of rhabdoms from individual crabs (n = 1), sampled at progressive timepoints as they widen during dark-adaptation (a), or narrow during light-adaptation (b), in daytime and after sunset. Red/blue outlines indicate mean area (μm^2) for each individual + standard deviation (gray edge outside mean outline). (c) Rhabdom cross-sectional areas (individual means ± standard deviation bars) are shown for eyes in various stages of adaptation between light (white filled points) and dark (gray to black filled points), during daytime (blue) and after sunset (red), and from dark to light during daytime (blue dashed line). White points at 180 min represent individuals that remained fully light-adapted until 15:00 (blue outline) and 00:00 (red outline) for comparison [Color figure can be viewed at wileyonlinelibrary.com]

A closer look at photoreceptor cell ultrastructure during light-adaptation revealed that rhabdom edges were surrounded by vesicles formed by pinocytosis (budding off) from the microvillar bases (Figure 9a). The cell somas of these eyes also contained many organelles including multivesicular bodies and multilamellar bodies involved with protein and lipid recycling and storage. When imaged in longitudinal

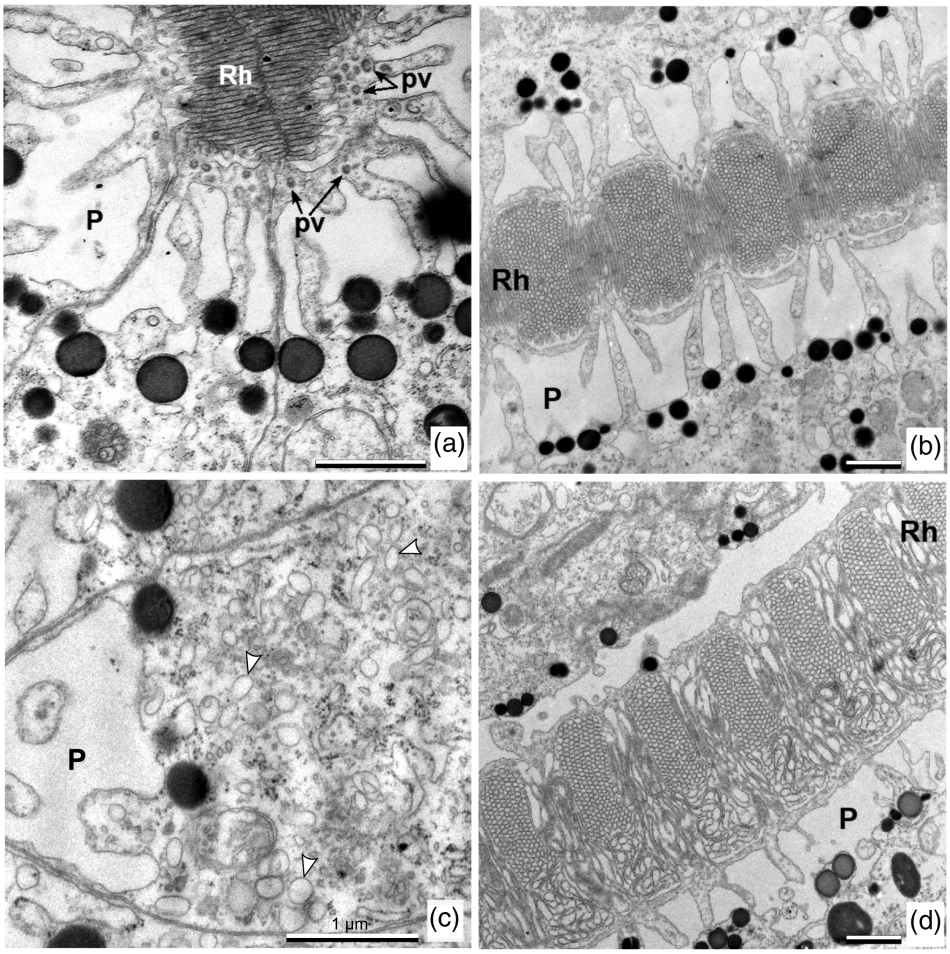

FIGURE 9 TEMs of (a) an ommatidium in cross-section during light-adaptation, midday, showing pinocytotic vesicles (pv) budding off from the edge of the rhabdom (Rh) to be transported into the cell soma via bridges in the palisade vacuole (P). (b) Longitudinal section through the distal rhabdom of a light-adapted eye, midday, showing the distinctive scallop-shaped edge. (c) At dusk, the photoreceptor soma of a light-adapted eye fills with endoplasmic reticulum tubules and vesicles containing opsin (white arrows), ready to travel through the palisade bridges and be incorporated into the growing rhabdom with onset of darkness. (d) Longitudinal section through a dark-adapted eye, midday, where all but one rhabdomere are in the process of reassembly with disordered microvillar membranes

section, fully light-adapted eyes had a distinctive scallop-shaped edge to the rhabdom (Figure 9b), whereas edges were straight in dark-adapted eyes. At dusk the photoreceptor somas fill with endoplasmic reticulum tubules and vesicles likely to contain opsin (Matsushita, Arikawa, & Eguchi, 1999), ready to be incorporated into the rhabdom with onset of darkness (Figure 9c). The palisade vacuoles of dark-adapted eyes tended to have more solid palisade vacuoles with fewer gaps than in light-adapted eyes (compare Figure 9b,d). When sectioned along the long axis of the ommatidia, some rhabdomeres were rarely observed in a state of degradation and turnover of the microvillar membranes, appearing disordered and loosely packed (Figure 9d).

3.6 | Length of photoreceptor cells and crystalline cones

Comparisons between the 3d synchrotron scan reconstructions of two eyes (one naturally light-adapted during daytime, the other dark-adapted until midnight) were made from seven horizontal tomogram slices, sampled at equivalent evenly-distributed positions along the vertical (dorso-ventral) axis of each eye (Figure 10a,b). The eyes were of similar overall dimensions (measurements in Supporting Information), but lengths of individual ommatidia varied substantially across each eye (78.2–510.4 µm), depending on the location in both vertical and horizontal planes, always shortening toward the edges of the eye. Areas of crystalline cone and photoreceptor cell regions (Figure 10b) were found to differ negligibly between the two eyes at all elevation angles (Figure 10c), although in the ventral eye, the ommatidia were slightly longer in the light-adapted eye. The proportion of each cell type area remained equivalent to the dark-adapted eye however (Figure 10d). Moving ventral to dorsal, the proportional area of eye tissue containing crystalline cones increased slightly in both eyes, ranging from 38.3 to 53.7%.

These data suggest that crystalline cones and photoreceptor cells do not change in absolute or proportional length between day and night. However, comparing two individuals with an unknown population variability, we have insufficient statistical power to dismiss an adaptative change in anatomy between day and night. Therefore, to allow statistical analysis we also measured lateral-facing ommatidia at the eye equator (0°) from a further 12 individuals. Their eyes, light-adapted at midday, or dark-adapted at midnight (n = 6), were compared with light microscopy (Figure 10e).

Rhabdom lengths (Figure 10f) differed considerably between individuals, ranging from 285.6 to 337.8 µm (both dark-adapted crabs). However, mean lengths were almost identical between the light-adapted and dark-adapted crabs (308.3 ± 13.6 and 307.3 ± 18.2 µm

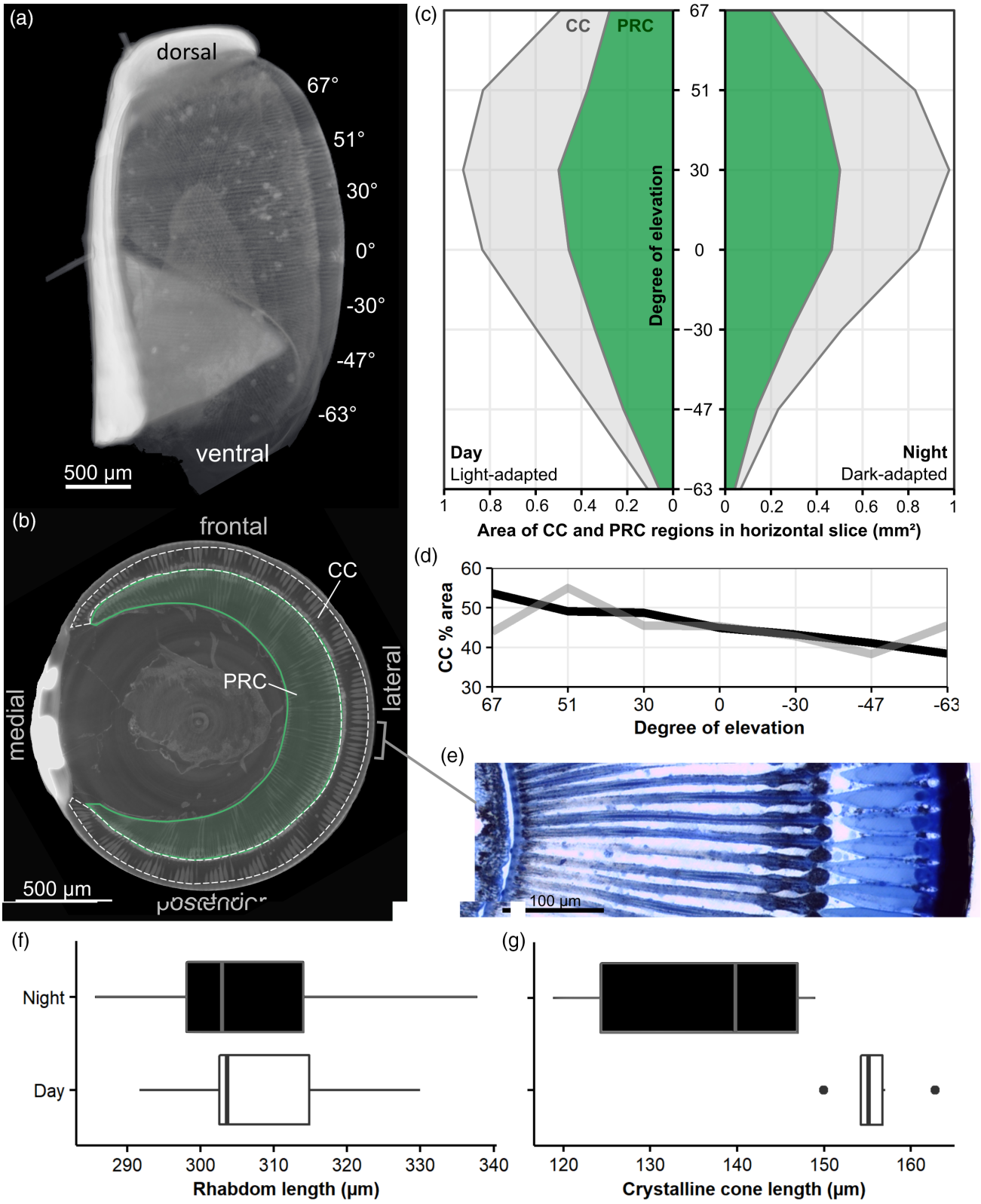

FIGURE 10 (a) Reconstructed synchrotron tomogram of a whole eye, frontal view. Horizontal slices were sampled at seven angles of elevation labeled along the eye's vertical (dorso-ventral) axis. (b) Annotated example slice from the eye equator (0°). Areas containing crystalline cones (CC) and photoreceptor cells (PRC) were measured and compared. (c) Areas (mm^2) of regions containing CC (gray) and PRC (green), in horizontal slices at seven angles of elevation along the eye are displayed for a light-adapted eye, midday (left) and a dark-adapted eye, midnight (right). (d) CC area as a percentage of the total eye tissue area (PRC + CC) in the light-adapted (gray) and dark-adapted eye (black), at seven angles of elevation. (e) Example light micrograph from a horizontal section across the eye equator (0°), from which lengths of six lateral-facing ommatidia were measured (line points to equivalent region in b). Rhabdom (f) and crystalline cone (g) lengths of midday light-adapted (white boxes) and midnight dark-adapted crabs (black boxes) measured from light micrographs ($n = 6$). Box contains the first to third quartiles with median line. Whiskers extend over the full range of measurements, outliers shown by points [Color figure can be viewed at wileyonlinelibrary.com]

respectively, Welch's *t*-test: $t_{[9]}$ = 0.109, p = .916). Crystalline cones (Figure 10g) were significantly longer in light-adapted crabs (155.7 ± 4.2 μm) than in dark-adapted crabs (136.0 ± 13.6 μm; Student's *t*-test, t_5 = 3.39, p < .007), conflicting with the result from our synchrotron data where no difference was measured between the two treatments (albeit n = 1).

4 | DISCUSSION

4.1 | Rhabdom changes

Rhabdom widening apparently provides the main structural mechanism in *A. tangeri* for increasing visual sensitivity at night, with cross-sectional area expanding by a factor of 5.6 from day to night. This would effectively adapt the eye from the very bright diurnal conditions in their tropical mudflat habitats to the gradual and predictable decreases in light levels at night. This appears to be a common mechanism across many arthropod taxa (Williams, 1982) and is also described as the primary adaptation strategy in *Ocypode* and *Grapsus*, for which the ultrastructural processes involved in microvillar membrane recycling by pinocytosis and reassembly have been closely examined (Nässel & Waterman, 1979; Blest et al., 1980; Stowe, 1980, 1981, 1983; Toh & Waterman, 1982; Stowe, Fukudome, & Tanaka, 1986; Toh, 1987, 1990; Arikawa et al., 1987; Matsushita et al., 1999; Rosenburg & Langer, 2001). Day-to-night rhabdom increases are reported for several other crab species (Figure 11), suggesting that nocturnal rhabdom widening may be widespread among intertidal brachyuran crabs. These increases range from a factor of 2.4 in *Callinectes sapidus* (Toh & Waterman, 1982) to 12.8 in *Ocypode ceratopthalmus* (Rosenburg & Langer, 2001), and rhabdoms can exceed 63 μm^2 in cross-sectional area in the night-adapted eye of *Hemigrapsus sanguineus penicillatus* (Matsushita et al., 1999). In comparison, *A. tangeri* does not appear to be as extreme in its rhabdom diameter cycling.

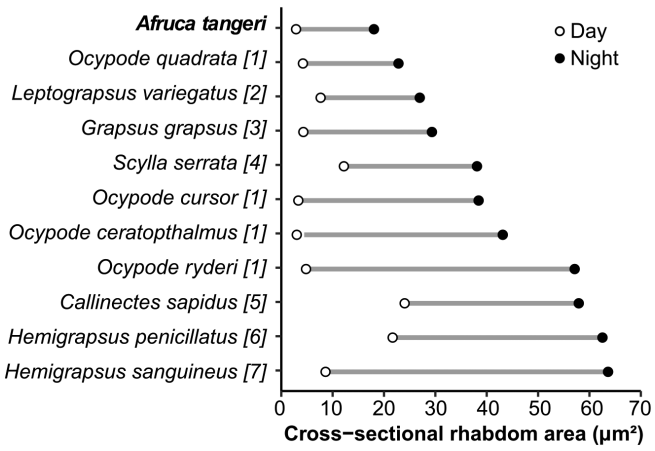

FIGURE 11 Mean cross-sectional area of rhabdoms of several intertidal brachyuran crab species between daytime light-adapted eyes (open circles) and night dark-adapted eyes (filled circles). Source indicated after species name: (1) Rosenburg & Langer, 2001, (2) Stowe, 1981 (3) Nässel & Waterman, 1979, (4) Leggett & Stavenga, 1981, (5) Toh & Waterman, 1982, (6) Toh, 1987, (7) Matsushita et al., 1999. Some of the published area measurements were calculated from diameters (d) using: Area = $\pi(\frac{d}{2})^2$

Rhabdom widening appears to be strongly linked to a circadian clock in *A. tangeri*. While mostly inhibited by bright light, the rhabdom only widens to its full extent when dark-adapted after sunset. Very similar findings have been reported for several other crabs (Arikawa, Morikawa, Suzuki, & Eguchi, 1988; Nässel & Waterman, 1979; Rosenburg & Langer, 2001). A conceivable evolutionary driver for this circadian control on rhabdom widening, may be the associated time and metabolic cost of synthesizing membrane for its microvillar elongations. Widening the rhabdom frequently to cope with short temporary periods of darkness during daytime may be too expensive to use as a strategy. Instead rhabdom diameter is strongly associated with the predictable decrease in light intensity at dusk and daily membrane turnover. From our observations of transitioning rhabdoms, this happens as described by Stowe (1980, 1981) in *Leptograpsus variegatus*. Our TEM data suggest that the partially widened rhabdoms of predark-adapted eyes during daytime can degrade via pinocytosis to a narrow light-adapted state within 30 min of exposure to bright light. However, dark adaptation is slower, our data suggesting that rhabdoms take several hours to widen in the dark, and only to the full extent after sunset. Further behavioral or electrophysiological work is now necessary to test how rhabdom changes affect the visual sensitivity of living crabs.

Increases in rhabdom length should also increase photopigment volume for light capture. As a dark-adaption strategy it has been observed only in few cases, including a tipulid fly (Williams, 1982), *Camponotus* ant (Menzi, 1987) and *Grapsus* crab (Nässel & Waterman, 1979). The 3d synchrotron datasets showed that rhabdom lengths vary substantially across the eye and differences of up to 18.2% existed between equivalent regions in equally-sized individuals of the same adaptation state. This may explain why Nässel and Waterman (1979) reported a 16% increase in the length of *Grapsus* crab rhabdoms from day to night, from four individuals. Our light micrograph measurements of equatorial eye regions indicate no rhabdom elongation from day to night in *A. tangeri*.

4.2 | Crystalline cones

There are substantial variations in ommatidial lengths across the eye (demonstrated by synchrotron data). Interestingly, crystalline cones appear to gradually lengthen in proportion to the photoreceptors in the dorsal hemisphere of the eye. This may be associated with regional specialization to facilitate a visual task, for example helping to optimize predator detection above the horizon, not required in the ventral eye, which is involved with detection of conspecifics (Layne, Land, & Zeil, 1997; Zeil & Hemmi, 2006). There was negligible difference in the proportional length of crystalline cones between the two tomograms, suggesting no shortening from day to night. Conflictingly, in our light-micrographs, the crystalline cones were shorter on average (~20 μm) at night when dark-adapted. Nocturnal crystalline cone shortening also occurs in *Camponotus* ants (Menzi, 1987) and brine

shrimp, *Artemia* (Nilsson & Odselius, 1981). We propose that the (very soft) crystalline cone cells in *A. tangeri* become shorter and wider at night, perhaps even maintaining constant cell volume, resulting in reduced focal length and wider proximal aperture, revealing a rhabdom that is also widening in diameter. These processes increase the acceptance angle and photon capture of each ommatidium, at the expense of spatial acuity (Warrant, 2008). The soft consistency of the crystalline cone cells means that they can deform during TEM sample preparation, so only eyes with straight cells were measured. However, to confirm our findings, further comparisons of a large sample of intact and minimally damaged eyes (scanned with CT/synchrotron) would be worthwhile.

4.3 | Distal pigment cells

Microscopy and X-ray synchrotron tomography of *A. tangeri* eyes indicate that pigment granules within the PPCs remained in fixed position from day to night and are thus unlikely to effectively moderate light flux to the photoreceptors below. This was surprising given that Fingerman (1970) measured substantial migrations of screening pigment in the fidder crab *Leptuca pugliator*. His method of measuring the width of the back-lit translucent area (crystalline cones and cornea) in comparison to the total eye width, using a light microscope, generated a rough ratio given the apparatus employed. Contrary to our own findings, his measurements strongly indicated a circadian distal movement of pigment into the crystalline cone region at night, showing that it retracts proximally again during daytime even in the absence of light. Fingerman's study did not identify the cells involved and it is possible that the pigment migration occured in the finer, low contrast SPCs (not examined in this study); or that shortening crystalline cones at night could gave an illusion of pigment migrations. Alternatively, our dissimilar data on *A. tangeri*, may simply be due to species-specific differences in this strategy (the two crabs are from a different subfamiles); differences in visual adaptation strategies are not unusual between related species of arthopods (Brown, 1961). It would be interesting to try and replicate his experiment with *A. tangeri*.

Distal pigment migrations in crustaceans are not uncommon. In the mud crab *Scylla serrata*, screening pigment migrates distally away from the distal rhabdom tip to a more dispersed arrangement between crystalline cones (Leggett & Stavenga, 1981). This was shown both histologically and in the living eye using an ophthalmascope, showing as a bright "iris" of pigment around the psuedopupil. Only seen after several hours of dark-adaptation at night, it was absent in the daytime or when light-adapted. In *A. tangeri*, although the deep pseudopupil widened, no change in appearance or eye shine was observed even after 3 hr dark-adaptation after sunset. Furthermore, TEMs revealed that the four PPCs encircling each crystalline cone make no contact in any adaptation state until the very proximal tip of the cones where they meet the rhabdom. They do not appear to actively constrict the proximal cone tract in bright light as they do in some nocturnal ants, for example (Menzi, 1987; Narendra, Alkaladi, Raderschall, Robson, & Ribi, 2013; Narendra, Greiner, Ribi, & Zeil, 2016). Diameter increases at night in the pupillary opening between PPCs were found to be unconvincingly small, with just a 1.15 μm mean diameter increase (19.7%) from light-adapted eyes at midday to dark-adapted eyes at midnight. This further dismisses distalpigment migrations as an adaptation strategy in this species.

4.4 | Acceptance angles

Rhabdom widening was accompanied by equivalent increases in the diameter of the lower crystalline cone tract, which tapered to match the diameter of the distal rhabdom in each treatment. As aperture diameter correlates directly with the size of the deep pseudopupil and resulting acceptance angles, we could measure the extent of aperture widening during dark adaptation via ophthalmoscopy of living eyes. Despite apparent lack of pigment migration in PPCs, after sunset acceptance angles increased 56.4% after 3 hr in the dark. Theoretical acceptance angles ($\Delta\rho$) for midday light-adapted eyes and midnight dark-adapted eyes, were calculated from our measurements of ommatidial dimensions using Equation (1), proposed by Snyder (1979),

$$\Delta\rho = \sqrt{\left(\frac{\lambda}{D}\right)^2 + \left(\frac{d}{f}\right)^2} \quad (1)$$

We used mean ommatidial measurements of lateral-facing facets at the eye equator (Table 4). Peak spectral sensitivity (λ_{max}) for *A. tangeri* is ~528 nm (Jordão et al., 2007), therefore this was used as the wavelength (λ) in our calculations. In the equatorial acute zone of the eye, spatial resolution is highest and facets are largest (Bagheri et al., 2020). Facet diameter (D), the distance between the centre point of adjacent facets at the cornea, was measured from light micrographs (n = 12). Focal length (f), the distance from the distal rhabdom tip to the nodal point of the corneal lens, was approximated to the length of the crystalline cone (slight error likely as precise location of nodal point was unknown).

Our calculations demonstrate that acceptance angle ($\Delta\rho$) doubles from 1.16 ± 0.04° in a midday light-adapted eye, to 2.23 ± 0.09° when dark-adapted at night. This is consistent with the 56.4% deep pseudopupil expansion observed with ophthalmoscopy and is a result of wider apertures and rhabdom tips, in addition to a slightly shorter focal length (crystalline cone) associated with dark-adapted eyes at

TABLE 4 Mean dimensions of *A. tangeri* eyes in a daytime light-adapted and midnight dark-adapted state (n = 6–8), used to calculate theoretical acceptance angles and optical sensitivity

	Light-adapted, midday	Dark-adapted, midnight
Facet diameter (D)	34 ± 3 μm	34 ± 3 μm
Rhabdom diameter (d)	2.0 ± 0.4 μm	4.8 ± 4.5 μm
Rhabdom length (l)	308 ± 14 μm	307 ± 18 μm
Focal length (f)	156 ± 4 μm	136 ± 14 μm
Acceptance angle ($\Delta\rho$)	1.16 ± 0.04°	2.23 ± 0.09°

night. A scaled diagrammatic summary of our anatomical findings (Figure 12) displays the mean measurements for crystalline cone and rhabdom changes in dark- and light-adapted eyes of *A. tangeri* between night and day.

Like the rhabdom, widening of the crystalline cone tip aperture appears to be under strong circadian control, remaining narrow during daytime even after 3 hr in the dark. Despite prolonged exposure to bright light after sunset, the predictable dark-adaptation process appeared to have partially begun in light-adapted eyes, as apertures were already slightly wider than their daytime size. These strong circadian effects on aperture dynamics, resulting in much wider acceptance angles at night, has also been demonstrated by ophthalmoscopy in *Scylla* crabs (Leggett & Stavenga, 1981) and the beetle *Tenebrio molitor* (Ro & Nilsson, 1993). In the fiddler crab, the aperture width of the crystalline cone tip helps to maintain a light-adapted state during daytime and prepare the eye for darkness at night.

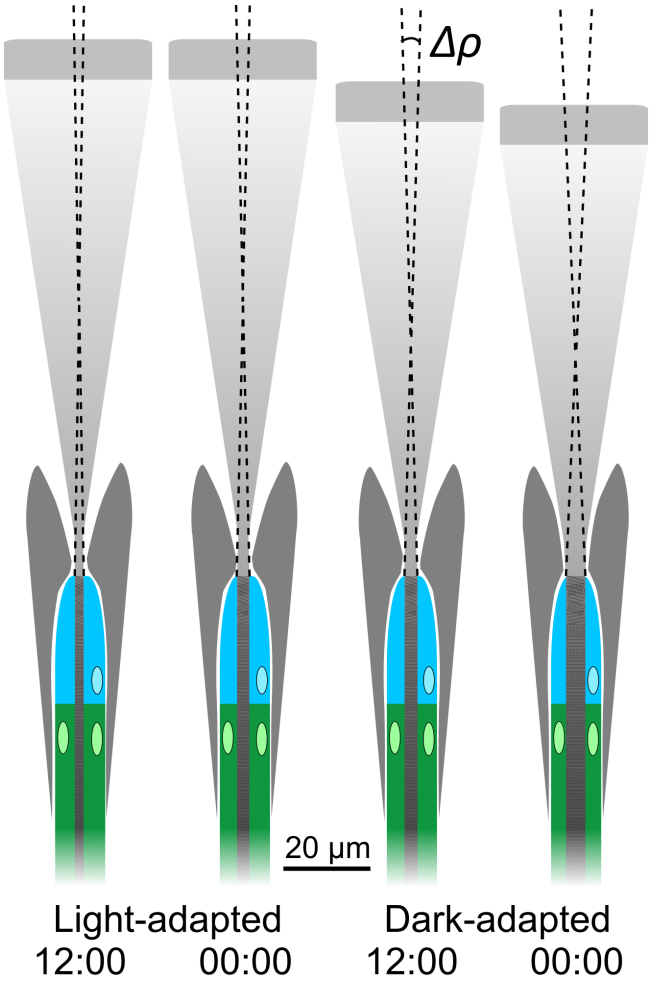

FIGURE 12 Summary of the ultrastructural differences observed in *A. tangeri* ommatidia in light- and dark-adapted eyes between midday and midnight. Dimensions of the crystalline cones and adjoining distal rhabdom tracts are to scale, with surrounding primary pigment cells (dark gray). Relative acceptance angles ($\Delta\rho$) are indicated by dotted lines through the crystalline cones [Color figure can be viewed at wileyonlinelibrary.com]

4.5 | Photoreceptor screening pigments

The ommatidial changes described thus far are slow and circadian and allow sensitivity adjustments to cope effectively with the regular and predictable changes in light levels between day and night. So how does the fiddler crab react to fluctuations in brightness during the daytime, for example when entering the burrow for short periods? Many insects such as dipteran flies, butterflies (Land & Nilsson, 2012) and ants (Narendra et al., 2016) use radial pigment migrations in the eye to react quickly to fluctuating light levels. Screening pigment granules contract inward to tightly encircle the rhabdom in bright light, then move away from the light path in darkness, functioning as a pupil. Though not widely reported in marine arthropods, it has been observed in the mantis shrimp *G. oerstedii* (King & Cronin, 1994a, 1994b), a horseshoe crab, *Limulus polyphemus* (Miller & Cawthon, 1974) and the amphipod *Paryhale hawaiensis* (Ramos et al., 2019), a diverse mix of arthropod taxa.

In light-adapted *A. tangeri* eyes fixed at midday, TEMs revealed ≤4.3% of pigment granules to be within the cytoplasmic palisade bridges and they did not resemble the distributions of light-adapted *G. oerstedii* eyes, in which radial pigment migrations occur (King and Cronin 1994b). Therefore, despite the presence of one or two granules occasionally located in bridges (examples found in all treatments); we did not find convincing evidence of effective radial screening pigment migrations within photoreceptors in this species. The palisades in light-adapted eyes appeared less solid in shape with larger gaps so this may explain the slightly greater number of granules therein. The travel distance through palisade bridges is very short (<3 µm) and there was concern about granules snapping back to dark-adapted positions during dissection and fixation. Eyes were dissected immediately into fixative using the method described by Alkaladi and Zeil (2014) to best preserve the pigment distributions in fiddler crabs, although anesthesia with ice was avoided as cold temperatures are known to disrupt radial pigment migrations in mantis shrimp (King & Cronin, 1994a, 1994b). We also tried dissecting light-adapted eyes straight into 70–80°C fixative, which has also been claimed historically to maintain true pigment distributions by instant protein denaturation (e.g., Knowles, 1950). Still, evidence of radial pigment migrations was not observed with this prep and it produced substandard tissue quality. Exposing dark-adapted eyes to light with the ophthalmoscope for 10 s also resulted in no change in deep pseudopupil diameter or appearance. Some change within this timeframe would be expected if radial pigment migration had occurred, as in mantis shrimp, these take 2–5 s under normal temperatures (King & Cronin, 1994a). This, plus the absence of any examples of light-induced radial screening pigment migration (as seen in other mentioned species) in any of our extensive library of *A. tangeri* eye TEMs, supports our conclusion that this is not a strategy used by this species.

The unchanging screening pigment distributions in the eye between light and dark, night and day, imply that the eye remains fully adapted to bright light even after periods in a dark burrow during daytime. While this may seem disadvantageous, a reason for this could be simply lack of necessity to dark-adapt during daytime. The habitats and lifestyles of some arthropods (e.g., flying insects) necessitate fast

visual adaptation, however the mudflat or sandy habitat is mostly free from large shady patches, except passing clouds. While sheltering from predators can be frequent, there is no requirement for vision inside the burrow. However, on exiting, it is extremely important that they can see well enough in the bright light to detect the presence of potential predators. Therefore, we believe effective daytime dark-adaptation is neither necessary nor beneficial to a fiddler crab. Similar ideas have been proposed by Leggett and Stavenga (1981) for a mud crab, *Scylla serrata* which may spend much of the daytime moving between dark refuges. Pigment migrations in the superposition eye of nocturnal moths keep it light-adapted during inactive daytimes spent in a dark refuge. This prepares the eye for flight in bright daylight in case the moth is suddenly discovered by a predator (Warrant & McIntyre, 1996).

4.6 | Optical sensitivity

To estimate the effect of physiological changes on the light-absorbing potential of the eye as it adapts from bright daylight to darkness at night, we calculated theoretical optical sensitivities (S) to white light using Equation (2) proposed by Warrant and Nilsson (1998),

$$S = \left(\frac{\pi}{4}\right)^2 D^2 \left(\frac{d}{f}\right)^2 \left(\frac{kl}{2.3 + kl}\right). \quad (2)$$

Again, mean measurements from lateral-facing facets at the eye equator were used (Table 4), including diameters (d) and lengths (l) of the rhabdoms, the size of the aperture through which light enters the eye, facet diameter (D) and focal length (f). The absorption coefficient (k) of the photoreceptor was assumed to be 0.0265 μm^{-1}, a typical value for crabs (Cronin & Forward, 1988). Optical sensitivity (S) of a light-adapted eye at midday was 0.096 ± 0.017 μm^2 sr. At night, due to the wider rhabdom and slightly shorter focal length, the light-gathering power of a dark-adapted eye is boosted to 0.704 ± 0.086 μm^2 sr, an estimated 7.4-fold increase in photon capture.

4.7 | Visual ecology

The flat habitat and ethology of fiddler crabs mean there is little need to adapt to darkness during daytime hours, and at night, darkness can be used to the crab's advantage. A lack of aerial predators means a safe extended foraging or mating time on warm evenings. By our own observations during the breeding season, male crabs continued to signal visually for at least 2 hr after sunset on warm nights, although acoustic signals via tapping the substrate or body with the major cheliped became more frequent as the evening progressed (also observed by Salmon & Atsaides, 1968; Wolfrath, 1993). Crabs were noted to be uncharacteristically bold at night and could be approached by torchlight, showing little concern about potential capture until the last few seconds (pers. obs., EB). This has also been noticed by Andalucían fishermen, to whom the males will occasionally lose their dominant claw. They are often collected after sunset when they are of more relaxed temperament (personal communication). *A. tangeri* activity is also constrained by declining surface temperatures in the evening and they retreat into burrows below 18°C (Wolfrath, 1993), meaning nocturnal foraging is restricted to summer months. To the human eye at least, as the light fades, the brilliant white claws become highly conspicuous against the dark mud background (Jordão & Oliveira, 2001) and courtship often occurs after sunset (von Hagen, 1962). Perhaps signaling activity after dusk in this species has driven selection for a highly reflective cheliped with uniform white colouration, at a potential cost of increased visibility to predators. Meanwhile, the rest of the body shows much temporal and spatial polymorphic variation within and between individuals, but relative to other fiddler crabs, is generally dull (Cummings et al., 2008).

We now know that while fiddler crabs will experience large increases in visual sensitivity around sunset, they will not fully dark-adapt during daytime and might struggle effectively to adjust to fluctuating light levels. When measuring responses to visual stimuli in these animals during future behavioral or electrophysiological experiments, it is very important to consider time of day and prior ambient lighting conditions. Further research will now investigate the extent to which rhabdom increases affect the relative sensitivity of the visual system of this species in these different adaptation states. There are also questions remaining about whether the metabolic cost of membrane production involved with rhabdom volume increases is offset by a slower temporal resolution. Although fast ultrastructural changes are visibly absent in *A. tangeri*, temporal summation might be used as an alternative strategy to increase sensitivity in short and temporary periods of darkness (Warrant, 1999).

ACKNOWLEDGMENTS

Many thanks to the electron microscopy team for technical support at the Wolfson Bioimaging Centre, Bristol and to José Ignacio Navas Triano at Instituto de Investigación y Formación Agraria y Pesquera Centro de Agua del Pino. Animal collection was carried out with the authorization of the Consejería de Medio Ambiente y Ordenación del Territorio de la Junta de Andalucía. We acknowledge the Paul Scherrer Institut, Villigen, Switzerland for provision of synchrotron radiation beamtime at the TOMCAT beamline X02DA of the SLS. Funding for the research was provided by The Royal Society. Thanks also go to Dr John Christy who provided valuable insight at the early stages of the study. This study was supported by The Royal Society (grant numbers UF140558 and RG150565).

CONFLICT OF INTEREST

The authors declare no conflict of interest.

AUTHOR CONTRIBUTIONS

Emelie A. Brodrick carried out the experiments, wrote the manuscript and produced figures and tables. Martin J. How conceived the project and provided initial ideas. Martin J. How and Nicholas W. Roberts supervised and supported the project and assisted in construction of the ophthalmoscope. Christian M. Schlepütz, Lauren Sumner-Rooney, &

Martin J. How scanned eye samples and reconstructed synchrotron tomograms, then assisted in writing of the related methods. Nicholas W. Roberts, Lauren Sumner-Rooney, & Martin J. How assisted with proofreads.

ETHICS APPROVAL

The experiments outlined herein were conducted in accord with UK legislation and with the ethical approval of Animal Welfare and Ethics Review Body at the University of Bristol, under UIN agreement number UB/18/070.

DATA AVAILABILITY STATEMENT

The data that support the findings of this study are available from the corresponding author upon reasonable request.

ORCID

Emelie A. Brodrick https://orcid.org/0000-0001-7349-1494
Christian M. Schlepütz https://orcid.org/0000-0002-0485-2708

REFERENCES

Alkaladi, A., & Zeil, J. (2014). Functional anatomy of the fiddler crab compound eye (*Uca vomeris*: Ocypodidae, Brachyura, Decapoda). *The Journal of Comparative Neurology*, *522*, 1264–1283. https://doi.org/10.1002/cne.23472

Altevogt, R., & von Hagen, H.-O. (1964). Über die Orientierung von *Uca tangeri* Eydoux im Freiland. *Zeitschrift für Morphol Und Ökologie der Tiere*, *53*, 636–656. https://doi.org/10.1007/BF00407731

Arikawa, K., Kawamata, K., Suzuki, T., & Eguchi, E. (1987). Daily changes of structure, function and rhodopsin content in the compound eye of the crab *Hemigrapsus sanguineus*. *Journal of Comparative Physiology. A*, *161*, 161–174. https://doi.org/10.1007/BF00615238

Arikawa, K., Morikawa, Y., Suzuki, T., & Eguchi, E. (1988). Intrinsic control of rhabdom size and rhodopsin content in the crab compound eye by a circadian biological clock. *Experientia*, *44*, 219–220. https://doi.org/10.1007/BF01941711

Bagheri, Z. M., Jessop, A.-L., Kato, S., Partridge, J. C., Shaw, J., Ogawa, Y., & Hemmi, J. M. (2020). A new method for mapping spatial resolution in compound eyes suggests two visual streaks in fiddler crabs. *The Journal of Experimental Biology*, *223*, 1–11. https://doi.org/10.1242/jeb.210195

Barnatan, Y., Sztarker, J., & Tomsic, D. (2019). Unidirectional optomotor responses and eye dominance in two species of crabs. *Frontiers in Physiology*, *1*, 586. https://doi.org/10.3389/fphys.2019.00586

Blest, A. D., Stowe, S., & Price, D. G. (1980). The sources of acid hydrolases for photoreceptor membrane degradation in a grapsid crab. *Cell and Tissue Research*, *205*, 229–244. https://doi.org/10.1007/BF00234682

Brown, F. A. T. H. W. (1961). The physiology of Crustacea. In T. H. Waterman (Ed.), *The physiology of Crustacea* (pp. 401–430). New York: Academic Press.

Chiou, T.-H., Cronin, T. W., Caldwell, R. L., & Marshall, J. (2005). Biological polarized light reflectors in stomatopod crustaceans. *Proceedings of SPIE - The International Society for Optical Engineering 5888*.

Cronin, T. W., & Forward, R. B. (1988). The visual pigments of crabs—I. spectral characteristics. *Journal of Comparative Physiology. A*, *162*, 463–478. https://doi.org/10.1007/BF00612512

Cummings, M. E., Jordão, J. M., Cronin, T. W., & Oliveira, R. F. (2008). Visual ecology of the fiddler crab, *Uca tangeri*: Effects of sex, viewer and background on conspicuousness. *Animal Behaviour*, *75*, 175–188. https://doi.org/10.1016/J.ANBEHAV.2007.04.016

Dag, O., Dolgun, A., & Konar, N. M. (2018). Onewaytests: An R package for one-way tests in independent groups designs. *The R Journal*, *10*, 175–199. https://doi.org/10.32614/rj-2016-023

De Moraes Vaz Batista Filgueira, D., Guterres, L. P., De Souza Votto, A. P., Vargas, M. A., Trindade, G. S., & Nery, L. E. M. (2010). Nitric oxide-dependent pigment migration induced by ultraviolet radiation in retinal pigment cells of the crab *Neohelice granulata*. *Photochemistry and Photobiology*, *86*, 1278–1284. https://doi.org/10.1111/j.1751-1097.2010.00787.x

Detto, T. (2007). The fiddler crab *Uca mjoebergi* uses colour vision in mate choice. *Proceedings of the Royal Society B: Biological Sciences*, *274*, 2785–2790. https://doi.org/10.1098/rspb.2007.1059

Eguchi, E., & Waterman, T. H. (1967). Changes in retinal fine structure induced in the crab *Libinia* by light and dark adaptation. *Zeitschrift für Zellforsch Und Mikroskopische Anatomie*, *79*, 209–229. https://doi.org/10.1007/BF00369286

Falkowski, M. (2017) *The spectral and temporal properties of fiddler crab photoreceptors in the context of predator avoidance*. (PhD Thesis). The University of Western Australia.

Fingerman, M. (1970). Circadian rhythm of distal retinal pigment migration in the fiddler crab, *Uca pugilator*, maintained in constant darkness and its endocrine control. *The Journal of Interdisciplinary Cycle Research*, *1*, 115–121. https://doi.org/10.1080/09291017009359210

Franceschini, N. (1972). Pupil and Pseudopupil in the compound eye of *Drosophila*. In *Information processing in the visual Systems of Anthropods* (pp. 75–82). Berlin Heidelberg: Springer.

Hemmi, J. M. (2005). Predator avoidance in fiddler crabs: 1. Escape decisions in relation to the risk of predation. *Animal Behaviour*, *69*, 603–614. https://doi.org/10.1016/j.anbehav.2004.06.018

How, M. J., Christy, J. H., Temple, S. E., Hemmi, J. M., Marshall, N. J., & Roberts, N. W. (2015). Target detection is enhanced by polarization vision in a fiddler crab. *Current Biology*, *25*, 3069–3073. https://doi.org/10.1016/j.cub.2015.09.073

How, M. J., Pignatelli, V., Temple, S. E., Marshall, N. J., & Hemmi, J. M. (2012). High e-vector acuity in the polarisation vision system of the fiddler crab *Uca vomeris*. *The Journal of Experimental Biology*, *215*, 2128–2134. https://doi.org/10.1242/jeb.068544

Jordão, J. M., Cronin, T. W., & Oliveira, R. F. (2007). Spectral sensitivity of four species of fiddler crabs (*Uca pugnax*, *Uca pugilator*, *Uca vomeris* and *Uca tangeri*) measured by *in situ* microspectrophotometry. *The Journal of Experimental Biology*, *210*, 447–453. https://doi.org/10.1242/jeb.02658

Jordão, J. M., & Oliveira, R. F. (2001). Major claws make male fiddler crabs more conspicuous to visual predators: A test using human observers. In *Advances in decapod crustacean research* (pp. 241–247). Netherlands: Springer.

King, C. A., & Cronin, T. W. (1994a). Investigations of pigment granule transport systems in *Gonodactylus oerstedii* (Crustacea: Hoplocarida: Stomatopoda) I. effects of low temperature on the pupillary response. *Journal of Comparative Physiology. A*, *175*, 323–329. https://doi.org/10.1007/BF00192991

King, C. A., & Cronin, T. W. (1994b). Investigations of pigment granule transport systems in *Gonodactylus oerstedii* (Crustacea: Hoplocarida: Stomatopoda) II. Effects of low temperature on pigment granule position and microtubule populations in retinular cells. *Journal of Comparative Physiology. A*, *175*, 331–342. https://doi.org/10.1007/BF00192992

Knowles, F. G. (1950). The control of retinal pigment migration in *Leander serratus*. *The Biological Bulletin*, *98*, 66–80. https://doi.org/10.2307/1538600

Land, M. F., & Nilsson, D.-E. (2012). *Animal Eyes*. Oxford, UK: Oxford University Press.

Latruffe, C., McGregor, P. K., & Oliveira, R. F. (1999). Visual signalling and sexual selection in male fiddler crabs *Uca tangeri*. *Marine Ecology Progress Series*, *189*, 233–240. https://doi.org/10.3354/meps189233

Layne, J., Land, M., & Zeil, J. (1997). Fiddler crabs use the visual horizon to distinguish predators from conspecifics: A review of the evidence. *Journal of the Marine Biological Association of the United Kingdom*, *77*, 43–54. https://doi.org/10.1017/s0025315400033774

Leggett, L. M. W., & Stavenga, D. G. (1981). Diurnal changes in angular sensitivity of crab photoreceptors. *Journal of Comparative Physiology. A*, *144*, 99–109. https://doi.org/10.1007/BF00612803

Legland, D. I. A.-C., & Andrey, P. (2016). MorphoLibJ: Integrated library and plugins for mathematical morphology with ImageJ. *Bioinformatics*, *32*, 3532–3534. https://doi.org/10.1093/BIOINFORMATICS

Ludolph, C., Pagnanelli, D., & Mote, M. I. (1973). Neural control of migration of proximal screening pigment by retinular cells of the swimming crab *Callinectes sapidus*. *The Biological Bulletin*, *145*, 159–170. https://doi.org/10.2307/1540356

Marone, F., & Stampanoni, M. (2012). Regridding reconstruction algorithm for real-time tomographic imaging. *Journal of Synchrotron Radiation*, *19*, 1029–1037. https://doi.org/10.1107/S0909049512032864

Matsushita, A., Arikawa, K., & Eguchi, E. (1999). Appearance of opsin-containing vesicles as rhabdomeric precursors and their incorporation into the rhabdom around dusk in the compound eye of the crab, *Hemigrapsus sanguineus*. *Zoological Science*, *16*, 25–34. https://doi.org/10.2108/zsj.16.25

Menzi, U. (1987). Visual adaptation in nocturnal and diurnal ants. *Journal of Comparative Physiology. A*, *160*, 11–21. https://doi.org/10.1007/BF00613437

Meyer-Rochow, V. B. (2001). The crustacean eye: Dark/ light adaptation, polarization sensitivity, flicker fusion frequency, and photoreceptor damage. *Zoological Science*, *18*, 1175–1197. https://doi.org/10.2108/zsj.18.1175

Miller, W. H., & Cawthon, D. F. (1974). Pigment granule movement in *Limulus* photoreceptors. *Investigative Ophthalmology*, *13*, 401–405.

Narendra, A., Alkaladi, A., Raderschall, C. A., Robson, S. K. A., & Ribi, W. A. (2013). Compound eye adaptations for diurnal and nocturnal lifestyle in the intertidal ant, *Polyrhachis sokolova*. *PLoS One*, *8*, e76015. https://doi.org/10.1371/journal.pone.0076015

Narendra, A., Greiner, B., Ribi, W. A., & Zeil, J. (2016). Light and dark adaptation mechanisms in the compound eyes of *Myrmecia* ants that occupy discrete temporal niches. *The Journal of Experimental Biology*, *219*, 2435–2442.

Nässel, D. R., & Waterman, T. H. (1979). Massive diurnally modulated photoreceptor membrane turnover in crab light and dark adaptation. *Journal of Comparative Physiology. A*, *131*, 205–216. https://doi.org/10.1007/BF00610429

Nilsson, D. E., & Odselius, R. (1981). A new mechanism for light-dark adaptation in the *Artemia* compound eye (Anostraca, Crustacea). *Journal of Comparative Physiology. A*, *143*, 389–399. https://doi.org/10.1007/BF00611178

Oliveira, R. F., & Custódio, M. R. (1998). Claw size, waving display and female choice in the European fiddler crab, *Uca tangeri*. *Ethology Ecology and Evolution*, *10*, 241–251. https://doi.org/10.1080/08927014.1998.9522855

Paganin, D., Mayo, S. C., Gureyev, T. E., Miller, P. R., & Wilkins, S. W. (2002). Simultaneous phase and amplitude extraction from a single defocused image of a homogeneous object. *Journal of Microscopy*, *206*, 33–40. https://doi.org/10.1046/j.1365-2818.2002.01010.x

Ramos, A. P., Gustafsson, O., Labert, N., Salecker, I., Nilsson, D. E., & Averof, M. (2019). Analysis of the genetically tractable crustacean *Parhyale hawaiensis* reveals the organisation of a sensory system for low-resolution vision. *BMC Biology*, *17*, 67. https://doi.org/10.1186/s12915-019-0676-y

Ro, A. I., & Nilsson, D. E. (1993). The circadian pupil rhythm in *Tenebrio molitor*, studied noninvasively. *Naturwissenschaften*, *80*, 186–189. https://doi.org/10.1007/BF01226382

Rosenburg, J., & Langer, H. (2001). Ultrastructural changes of Rhabdoms of the eyes of *Ocypode* species in relation to different regimes of light and dark adaptation. *Journal of Crustacean Biology*, *21*, 345–353.

Salmon, M., & Atsaides, S. P. (1968). Visual and acoustical signalling during courtship by fiddler crabs (genus *Uca*). *American Zoologist*, *8*, 623–639.

Schindelin, J., Arganda-Carreras, I., Frise, E., Kaynig, V., Longair, M., Pietzsch, T., … Cardona, A. (2012). Fiji: An open-source platform for biological-image analysis. *Nature Methods*, *9*, 676–682. https://doi.org/10.1038/nmeth.2019

Shih, H. T., Ng, P. K. L., Davie, P. J. F., Schubart, C. D., Türkay, M., Naderloo, R., Jones, D., … Liu, M-Y. (2016). Systematics of the family Ocypodidae Rafinesque, 1815 (Crustacea: Brachyura), Based on phylogenetic relationships, With a reorganization of subfamily rankings and a review of the taxonomic status of *Uca* Leach, 1814, *sensu lato* and its subgen. *The Raffles Bulletin of Zoology*, *64*, 139–175.

Smithers, S. P., Roberts, N. W., & How, M. J. (2019). Parallel processing of polarization and intensity information in fiddler crab vision. *Science Advances*, *5*, eaax3572. https://doi.org/10.1126/sciadv.aax3572

Smolka, J., & Hemmi, J. M. (2009). Topography of vision and behaviour. *The Journal of Experimental Biology*, *212*, 3522–3532. https://doi.org/10.1242/jeb.032359

Snyder, A. W. (1979). Physics of vision in compound eyes. In H. Autrum (Ed.), *Handbook of sensory physiology*, V11/6a (pp. 225–313). Berlin, Heidelberg: Springer.

Stampanoni, M., Groso, A., Isenegger, A., Mikuljan, G., Chen, Q., Bertrand, A., … Abela, R. (2006). Trends in synchrotron-based tomographic imaging: The SLS experience. *Proceedings of SPIE - The International Society for Optical Engineering 6318* (63180M).

Stansbury, M. S., & Moczek, A. P. (2013). The evolvability of arthropods. In *Arthropod biology and evolution: Molecules, development, morphology* (pp. 479–493). Berlin Heidelberg: Springer-Verlag.

Stowasser, A., Owens, M., & Buschbeck, E. K. (2017). Giving invertebrates an eye exam: An ophthalmoscope that utilizes the autofluorescence of photoreceptors. *The Journal of Experimental Biology*, *220*, 4095–4100. https://doi.org/10.1242/jeb.166629

Stowe, S. (1980). Rapid synthesis of photoreceptor membrane and assembly of new microvilli in a crab at dusk. *Cell and Tissue Research*, *211*, 419–440. https://doi.org/10.1007/BF00234397

Stowe, S. (1981). Effects of illumination changes on rhabdom synthesis in a crab. *Journal of Comparative Physiology. A*, *142*, 19–25. https://doi.org/10.1007/BF00605472

Stowe, S. (1983). Phagocytosis of rhabdomeral membrane by crab photoreceptors (*Leptograpsus variegatus*). *Cell and Tissue Research*, *234*, 463–467. https://doi.org/10.1007/BF00213782

Stowe, S., Fukudome, H., & Tanaka, K. (1986). Membrane turnover in crab photoreceptors studied by high-resolution scanning electron microscopy and by a new technique of thick-section transmission electron microscopy. *Cell and Tissue Research*, *245*, 51–60. https://doi.org/10.1007/BF00218086

Toh, Y. (1987). Diurnal changes of rhabdom structures in the compound eye of the grapsid crab, *Hemigrapsus penicillatus*. *Journal of Electron Microscopy*, *36*, 213–223. https://doi.org/10.1093/oxfordjournals.jmicro.a050627

Toh, Y. (1990). Diurnal changes in the cytoplasmic organelles of the retinular cell in the compound eye of the grapsid crab, *Hemigrapsus penicillatus*. *Journal of Electron Microscopy*, *39*, 492–500. https://doi.org/10.1093/oxfordjournals.jmicro.a050843

Toh, Y., & Waterman, T. H. (1982). Diurnal changes in compound eye fine structure in the blue crab *Callinectes*. 1. Differences between noon and midnight retinas on an LD 11: 13 cycle. *Journal of Ultrastructure Research*, *78*, 40–59. https://doi.org/10.1016/S0022-5320(82)80012-9

Vargas, M. A., Geish, M. A., Maciel, F. E., Cruz, B. P., de Moraes Vaz Batista Filgueira, D., de Jesus Ferreira, G., … Allodi, S. (2010). Influence of the dark/light rhythm on the effects of UV radiation in the eyestalk of the crab *Neohelice granulata*. *Comparative Biochemistry & Physiology—C Toxicology and Pharmacology*, *151*, 343–350. https://doi.org/10.1016/j.cbpc.2009.12.011

von Hagen, H.-O. (1962). Freilandstudien zur Sexual und Fortpflanzungs-Biologie von *Uca tangeri* in Andalusien. *Zeitschrift für Morphol. Und Ökologie der Tiere*, *51*, 611–725.

Warrant, E. (2008). Nocturnal vision. In R. Masland & T. Albright (Eds.), *The senses: A comprehensive reference* (Vol. 2: Vision II, pp. 53–86). San Diego: Elsevier.

Warrant, E. J. (1999). Seeing better at night: Life style, eye design and the optimum strategy of spatial and temporal summation. *Vision Research*, *39*, 1611–1630. https://doi.org/10.1016/S0042-6989(98)00262-4

Warrant, E. J., & McIntyre, P. D. (1996). The visual ecology of pupillary action in superposition eyes. *Journal of Comparative Physiology. A*, *178*, 75–90. https://doi.org/10.1007/BF00189592

Warrant, E. J., & Nilsson, D. E. (1998). Absorption of white light in photoreceptors. *Vision Research*, *38*, 195–207. https://doi.org/10.1016/S0042-6989(97)00151-X

Williams, D. S. (1982). Ommatidial structure in relation to turnover of photoreceptor membrane in the locust. *Cell and Tissue Research*, *225*, 595–617. https://doi.org/10.1007/BF00214807

Wolfrath, B. (1993). Observations on the behaviour of the European fiddler crab *Uca tangeri*. *Marine Ecology Progress Series*, *100*, 111–118.

Zeil, J., & Hemmi, J. M. (2006). The visual ecology of fiddler crabs. *Journal of Comparative Physiology. A*, *192*, 1–25. https://doi.org/10.1007/s00359-005-0048-7

SUPPORTING INFORMATION

Additional supporting information may be found online in the Supporting Information section at the end of this article.

How to cite this article: EA Brodrick, NW Roberts, L Sumner-Rooney, CM Schlepütz, MJ How. Light adaptation mechanisms in the eye of the fiddler crab *Afruca tangeri*. *J Comp Neurol*. 2021;529:616–634. https://doi.org/10.1002/cne.24973